(12)

TGAL-85-10

SEISMIC EVENT LOCATIONS USING MULTIPLE PHASES

A. C. Chang
Teledyne Geotech Alexandria Laboratories
314 Montgomery Street
Alexandria, Virginia 22314-1581

NOVEMBER 1985

FINAL TECHNICAL REPORT:
ARPA ORDER NO: 4435
PROJECT TITLE: Enhanced Location Using Multiple Arrivals
CONTRACT: F08606-85-C-0031

Approved for Public Release; Distribution Unlimited.

Prepared for:
DEFENSE ADVANCED RESEARCH PROJECTS AGENCY
1400 Wilson Boulevard
Arlington, VA 22209

Monitored By:
AFTAC/TGR
Patrick AFB
Florida 32925-6001

The views and conclusions contained in this report are those of the authors and should not be interpreted as representing the official policies, either expressed or implied, of the Defense Advanced Research Projects Agency or the U.S. Government.

UNCLASSIFIED
SECURITY CLASSIFICATION OF THIS PAGE

AD-A177 912

REPORT DOCUMENTATION PAGE

Form Approved
OMB No 0704 0188
Exp Date Jun 30, 1986

1a REPORT SECURITY CLASSIFICATION Unclassified	1b RESTRICTIVE MARKINGS
2a SECURITY CLASSIFICATION AUTHORITY	3 DISTRIBUTION / AVAILABILITY OF REPORT Approved for public release; distribution unlimited.
2b DECLASSIFICATION / DOWNGRADING SCHEDULE	
4 PERFORMING ORGANIZATION REPORT NUMBER(S) TGAL-85-10	5 MONITORING ORGANIZATION REPORT NUMBER(S)
6a NAME OF PERFORMING ORGANIZATION Teledyne Geotech Alexandria Laboratories 6b OFFICE SYMBOL (If applicable)	7a NAME OF MONITORING ORGANIZATION AFTAC/TGR
6c ADDRESS (City, State, and ZIP Code) 314 Montgomery Street Alexandria, VA 22314	7b ADDRESS (City, State, and ZIP Code) Patrick Air Force Base Florida 32925-6001
8a NAME OF FUNDING / SPONSORING ORGANIZATION DARPA 8b OFFICE SYMBOL (If applicable) GSD	9 PROCUREMENT INSTRUMENT IDENTIFICATION NUMBER F08606-85-C-0031
8c ADDRESS (City, State, and ZIP Code) 1400 Wilson Blvd. Arlington, VA 22209	10 SOURCE OF FUNDING NUMBERS PROGRAM ELEMENT NO: 62714E PROJECT NO: DT/5128 TASK NO: WORK UNIT ACCESSION NO:
11 TITLE (Include Security Classification) Seismic Event Locations Using Multiple Phases	
12 PERSONAL AUTHOR(S) A. C. Chang	
13a TYPE OF REPORT Final 13b TIME COVERED FROM Mar 85 TO Nov 85	14 DATE OF REPORT (Year, Month, Day) 851130 15 PAGE COUNT 56
16 SUPPLEMENTARY NOTATION	

17 COSATI CODES		
FIELD	GROUP	SUB-GROUP
08	11	
17	10	

18 SUBJECT TERMS (Continue on reverse if necessary and identify by block number)
seismic location; Nevada Test Site; regional phases; simultaneous inversions; inter-station correlation

19 ABSTRACT (Continue on reverse if necessary and identify by block number)

This work evaluates the utility of a travel time Covariance Matrix Method (COVMTX) for the improvement of the location of seismic events at regional distances using both Pn and Pg arrival times. The method is tested using 47 NTS events drawn from the Center for Seismic Studies (CSS) data base. Correlations between Pn and Pg travel time residuals are determined for the data set.

We determined that the correlation coefficient between the Pn travel time residuals at two stations follows the form

$$\rho_{P_n} = A_{P_n} \exp\left[\frac{-r_{ij}^2}{\Delta^2}\right]$$

(Continued)

20 DISTRIBUTION / AVAILABILITY OF ABSTRACT ☒ UNCLASSIFIED/UNLIMITED ☐ SAME AS RPT ☐ DTIC USERS	21 ABSTRACT SECURITY CLASSIFICATION Unclassified
22a NAME OF RESPONSIBLE INDIVIDUAL Capt. Vincent L. Sortman	22b TELEPHONE (Include Area Code) (305) 494-5263 22c OFFICE SYMBOL TGR

DD FORM 1473, 84 MAR — 83 APR edition may be used until exhausted. All other editions are obsolete.

SECURITY CLASSIFICATION OF THIS PAGE
UNCLASSIFIED

(19. Continued)

with a similar form for the correlation coefficient ρ_{P_g} between the Pg travel time residuals, and that $\rho_{P_n} = 0$ when $r_{ij} = 3°$ and that $\rho_{P_g} = 0$ when $r_{ij} = 2°$. Standard errors of Pn and Pg residuals were also determined to be $\sigma_{P_n} = 1.7$ sec and $\sigma_{P_g} = 3.0$ sec.

The correlation of Pn and Pg times, $\rho_{P_nP_g}$, for signals received at the same station from the same event was found to be very poor, less than 0.3 in all computations.

Using these determined values for ρ and σ, we have relocated and compared 47 NTS explosions using six different options. The Covariance Matrix Method did not improve the results as we hoped, possibly because the systematic bias due to the clustering of stations is small for the particular network of stations used in the relocation. Nevertheless, the method is still valuable because we must weight each signal differently, especially when multiple phases are used, and the values of σ_{P_n} and σ_{P_g} may be used to compute the relative weights for these two phases.

The Simultaneous Inversion Method often resulted in erroneous depth estimates, because the inversion for the depth dependent terms a_{P_n} and a_{P_g} in the linear travel time formula

$$t = a + b\Delta$$

may end up with some unacceptable values. By restricting the inversion for the a coefficients, the relocation resulted in the best results. This restriction is similar to the Successive Determinations Method devised by Chang et al. (1981), because it only improves the velocities or the b coefficients. This result suggests that a successive determinations approach may be very useful in locations using later phases, especially phases like S, PP, etc., where large local variations in travel times are noted but are unpredictable prior to the location.

TABLE OF CONTENTS

TABLE OF CONTENTS CONTINUED

LIST OF FIGURES

LIST OF TABLES

1. INTRODUCTION

1.1. Scope of the Project

The primary objective of this research was to develop methods to increase the accuracy of locating the hypocenters of seismic events. Many workers have tried to develop such methods in the past, but they have had only limited success. The main reason is that the Earth is laterally heterogeneous, so that locating events using a "standard" travel time formula or table results in limited accuracy. The accuracy of location estimates varies widely because of regional deviations from the standard model, the geographical distribution of seismic stations, and the variety of structures under those stations.

Seismic events are located primarily by using the teleseismic P phase and the crustal phases Pn and Pg. Occasionally, later phases such as pP, PKP and PcP are used. Later phases are difficult to use, partly because reliable travel time tables have not been developed for them, and partly because the lateral heterogeneity may have greater influence on them. Consequently, when later phases are used along with P, they should be weighted so that the poorly defined later phases are given less weight in the least squares solution than are the well defined phases such as P.

Chang et al. (1983) developed the Covariance Matrix Method (COVMTX), where each observed phase is properly weighted and where the influence of station bias due to the nonuniform distribution of of stations is removed by introducing a covariance matrix into the conventional least squares formula. However, inter-station correlation coefficients of seismic phases other than teleseismic P have not been determined, so the effectiveness of the method has not been thoroughly tested. The objective of this research is to determine the inter-station correlation coefficients of Pn and Pg arrival times and then include them in location programs so that the effectiveness of the COVMTX method can be evaluated.

1.2. History of Developing Location Programs

1.2.1. Development of ACLOC Method

The fact that the Earth is laterally heterogeneous can best be demonstrated by a display of true travel time residuals as a function of azimuth, as in the top diagram of Figure 1. Travel time residuals are caused by four major factors: (a) error in reading the signal arrival time, (b) error in clock times, (c) error in the seismic location and origin time, and (d) the lateral heterogeneity of the Earth. True travel time residuals can be determined using events with known location and origin time, such as nuclear explosions, so the error in location and origin time for these events is zero. Clock and reading errors can be minimized by careful operational procedures. True travel time residuals are then calculated with respect to a standard Earth model in the form of $T_{obs} - T_{calc}$, so that a positive residual (+) means that the observed travel time is greater than that predicted with a theoretical model, and a negative (-) residual means that the observed travel time is less than that predicted using the model. We choose as an example the nuclear explosion Carpetbag (37.129N, 116.083W), which took place at the Nevada Test Site. True travel time residuals for this event were computed with respect to Herrin's 1968 travel time table. Each ring in Figure 1 represents a 20 degree spacing in epicentral distance. Within the northeast quadrant of this figure we see stations in North America, with some late stations to the north of NTS within 20 degrees, but also early arrivals for stations in the Canadian shield. In the same quadrant and near 80 degrees distance, we see stations from Europe, with mixtures of early and late arrivals closely spaced. In the southeast quadrant we see stations ranging from Mexico to Chile in a curved line, mostly late arrivals reflecting the low velocity tectonic subduction regions in South America, especially from Peru to Chile. In the southwest quadrant, two closely spaced arrivals near 60° range are stations in Hawaii. In the northwest quadrant the effects of the low velocity tectonic regions of North

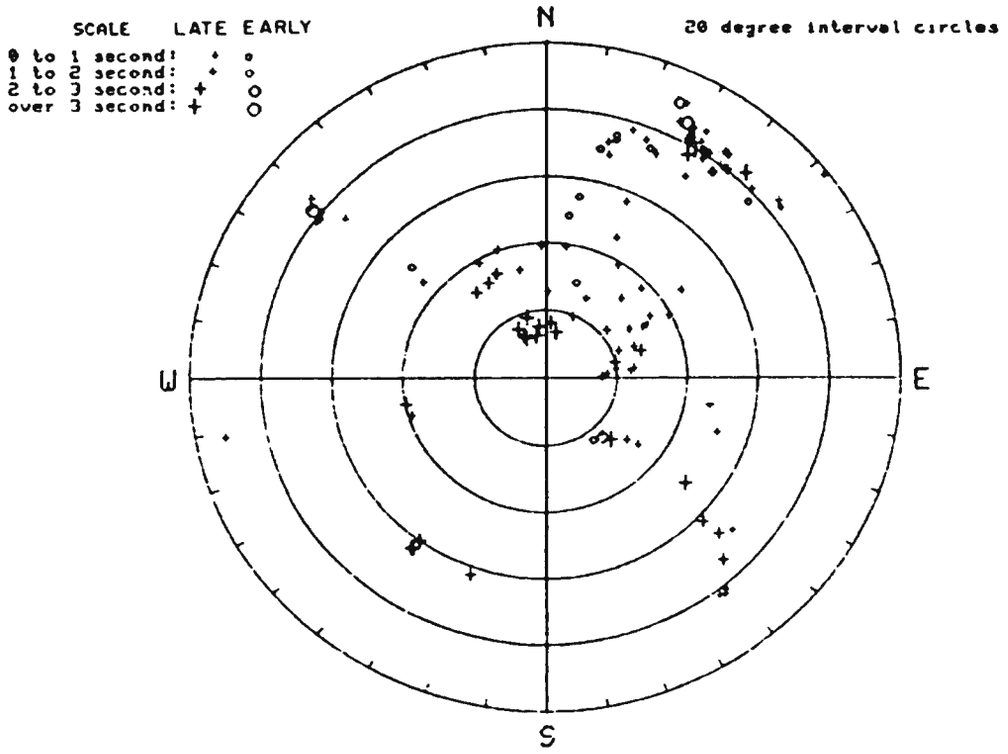

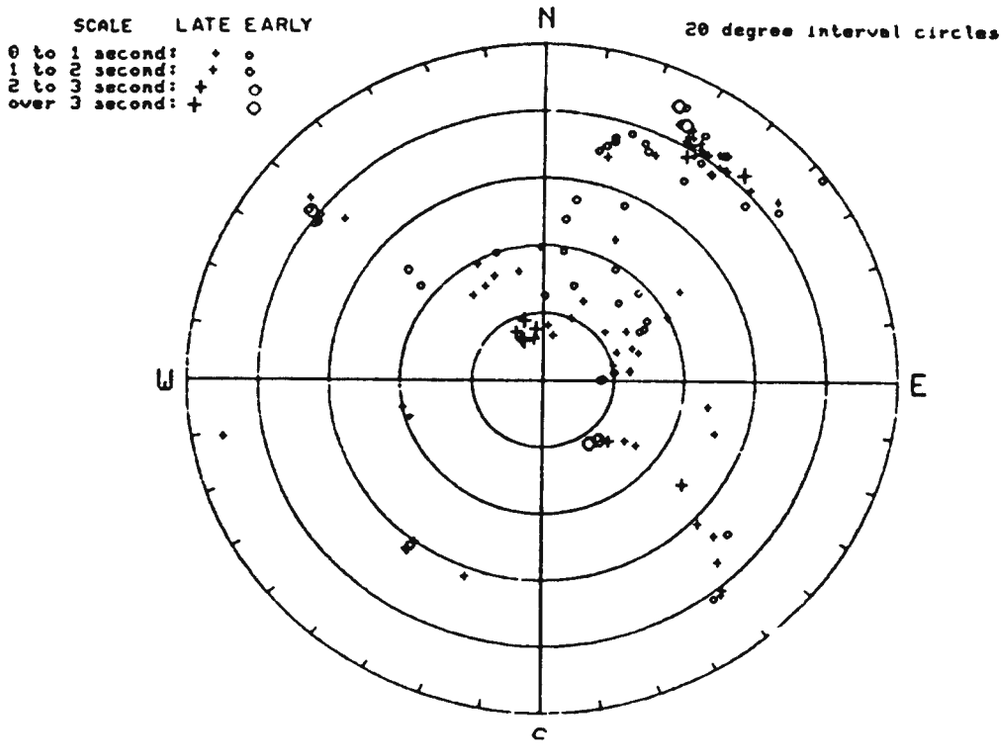

Figure 1 Comparison of true travel time residuals before and after using the ACLOC method.

America extending into Alaska are evident. Of special interest in this quadrant is the early arrival from Seoul sandwiched by two late arrivals from Japan and Korea.

In an attempt to correct for the earth's lateral heterogeneities, we devised a new method to compute travel times (Chang et al. 1983). In this method, called ACLOC, travel times are computed in a composite manner. Approximately 20 earth models were used to compute half-ray travel time tables. The complete ray-path travel time is computed by adding the two half-ray travel times for the source region and the station region, so many different combinations of half-rays are possible. In order to automate the procedure, one model is assigned to each geographic region (Flinn et al. 1965). The effectiveness of this method can be demonstrated by examining the true travel time residuals of the Carpetbag event shown in the bottom diagram of Figure 1. In comparison with the top diagram in Figure 1, one can see that the residuals are slightly reduced in magnitude, and in many regions the positive and negative residuals are intermixed, indicating that the systematic geographical biases in the travel times have been removed. Somewhat improved results can be observed in North America, South America, Hawaii, Alaska, etc. Results for arrivals from Europe are somewhat uncertain, suggesting the need for more detailed study of this region.

1.2.2. The Covariance Matrix Method (COVMTX)

Following the ACLOC method, Chang et al. (1983) devised a method to reduce the effect on seismic event locations of nonuniform distributions of detecting stations. As is obvious from Figure 1, seismic stations typically are not evenly distributed geographically. If stations are clustered in a particular region that is either early or late, then the least squares solution for the location may be influenced by the clustered stations, resulting in a systematic bias.

In order to reduce the effect of clustering bias we developed the Covariance Matrix Method (COVMTX). Assuming that successive corrections to the initial location are made

using the linearization of the travel time curve

$$\underline{\delta t} = \mathbf{B}(\underline{x} - \underline{x}_0) + \underline{\varepsilon} \tag{1}$$

where $\underline{\delta t}$ is the N x 1 vector of travel time residuals, $\underline{x}_0$ is the location determined during the previous iteration, and **B** is the N x 4 matrix of derivatives of the travel time residuals with respect to the 4 x 1 location coordinate vector $\underline{x} = (t_0, \theta, \phi, z)$ containing the origin time, latitude, longitude, and depth coordinates. The N x 1 error vector $\underline{\varepsilon}$ is assumed to be a Gaussian, zero mean, random vector with a covariance matrix given by

$$\mathrm{cov}(\underline{\varepsilon}) = \mathbf{E}\underline{\varepsilon}\underline{\varepsilon}' = \sigma_0^2\mathbf{\Sigma} \tag{2}$$

where σ_0^2 is an unknown proportionality constant. The matrix $\mathbf{\Sigma}$ is expressed in the form

$$\mathbf{\Sigma} = \mathbf{D}_\sigma\mathbf{R}\mathbf{D}_\sigma \tag{3}$$

where $\mathbf{D}_\sigma = (\sigma_1,\sigma_2,...,\sigma_N)$ is a diagonal matrix containing standard errors, and $\mathbf{R} = \{\rho_{ij},\ i,j = 1,..., N\}$, where ρ_{ij} is the correlation coefficient of stations i and j in terms of distance and the observed phases at stations i and j. The diagonal elements of the matrix **R** are of course set to 1.0. The method is a modification of Julian's method (1973), where the matrix $\mathbf{D}^2$ is a diagonal matrix containing the variance of the signal. By modifying $\mathbf{D}^2$ the form of equation (3), we intend to take into account : (a) inter-station arrival time correlation coefficients (for a single seismic phase), which are designed to remove the location bias due to the clustering of stations in a small vicinity, (b) weights assigned to each signal on the basis of the variance of the travel time for that seismic phase, and (c) inter-phase arrival time correlation coefficients (e.g., the correlation between Pn and Pg residuals at the same station). Using the COVMTX method it is now possible to use a mixture of phases and to counter-balance the clustering of stations in the seismic event location estimate. But in order to use multiple seismic phases, it will be necessary to determine the inter-station correlation coefficients of each phase as a function of the separation between stations as well as the inter-phase correlation coefficients for all pairs of phases.

1.2.3. Locations Using Regional Phases

In addition to teleseismic P, the phases Pn and Pg are often used in locating seismic events. Because these phases are observed in the distance range from zero to 10 degrees, they are often called regional or crustal phases. Other regional phases such as P^*, Sn, Sg, S^*, and Lg are seldom used. Because Pn and Pg have higher travel time velocity gradients than teleseismic P, it was generally thought that greater accuracy could be obtained by using them. But since the lateral heterogeneity of the Earth is also greater in the crust and upper mantle, standard errors of these phases are greater than P, resulting in no significant improvement in location accuracy.

Chang and Racine (1979) investigated the possibility of using local crustal models in the location procedure. In their program, about 35 crustal models were installed for the purpose of computing travel times of Pn and Pg. Each arrival phase was assigned a crustal model, so that one could use a model suitable for each source to station path. The results of this experiment, compared to the conventional method of using one standard table, were only marginally better. They speculated that the arbitrary selection of a crustal model by an analyst might not adequately describe the particular path, resulting in additional error.

Both Pn and Pg travel times are linear in a time-distance plot. By plotting travel times of Pn and Pg, Chang et al. (1981) showed that not only are the travel-time relations linear, but that the least square estimates of these relations for Pn and Pg vary from one event to another. Based on this result, Chang et al. (1981) designed two methods. The first method is the Successive Determinations Method (SUCCESS), in which the program first locates the event, computes the Pn and Pg velocities on the basis of this location, re-locates the event using these newly determined velocities, and then repeats the process. The second method is called the

Simultaneous Inversion Method (SIMUL), where the corrections to travel time curves and to the event locations are computed simultaneously rather than successively. Results showed that both methods decreased location errors from about 7 km to 4 km on the average.

1.3. Research Objectives

In order to use arrivals of all types of phases in seismic event location, we must use the COVMTX method to give proper weighting to each observation. For this purpose we must evaluate the inter-station correlation coefficient of each phase as a function of the separation between stations, and we must also evaluate the inter-phase correlation coefficients (at a single station) for all pairs of phases. Since the most commonly used phases other than P are Pn and Pg, our goal is to implement the use of these two phases in the location program and evaluate the results. To achieve this goal, we must accomplish the following :

(1) Determine the inter-station correlation coefficients ρ_{P_n} and ρ_{P_g} as a function of the separation between stations.

(2) Determine the standard deviations σ_{P_n} and σ_{P_g}. Determine the correlation of Pn and Pg recorded at the same station for the same event, $\rho_{P_nP_g}$.

(3) Implement these values in the location program and evaluate the result. Since the SIMUL and COVMTX methods can be used together, the evaluation shall test various combinations of these two options, i.e. with/without the COVMTX method, and with/without the SIMUL method.

2. COMPUTATION OF CORRELATION COEFFICIENTS OF ARRIVAL TIME RESIDUALS BETWEEN STATIONS

2.1. Data Base

The Explosion Data Base (INGRES database "SHTRPT") in the Center for Seismic Studies (CSS) was used to extract NTS shot arrival times. The Explosion Data Base contains about 90 NTS shot reports where shot names, arrivals, yields, areas and dates are stored in separate database files. However, not all of the events have arrival time files. We extracted a total of 47 events from this database. Table I lists the events and coordinates used, and Figure 2 shows the locations of these events. The events are grouped into four regions: Yucca Flat, Pahute Mesa, Rainier Mesa, and Frenchman Flat. Events in each group are located within 20 kilometers of each other, so they are considered as a group to compute correlation coefficients.

After extracting those events in groups, they are re-located by using J-B travel time tables and restricting all four hypocentral coordinates : latitude, longitude, depth and time. The residuals thereby obtained relative to the true locations, which we shall refer to as the "true" residuals, are stored in four groups of travel time residual files. These files are then used to compute correlation coefficients for Pn and Pg residuals as a function of the separation between stations.

We computed the correlation coefficients of Pn and Pg using these four groups, but since some groups have a very small number of events, the computations were repeated using combinations of groups, i.e., combining Pahute Mesa and Rainier Mesa events, combining Frenchman Flat and Yucca Flat events, and using all events.

TABLE I

LIST OF NTS EVENTS USED IN THE EXPERIMENT

Yucca Flat Events

No.	Name	Latitude	Longitude	Depth	Orig. Time
1	Aardvark	37.065	-116.030	4.4	19 00 00.1
2	Acushi	37.047	-116.021	2.6	18 30 00.1
3	Agouti	37.047	-116.034	2.6	18 00 00.1
4	Armadilo	37.044	-116.039	2.4	16 30 00.1
5	Auk	37.078	-116.009	4.6	20 03 00.0
6	Bilby	37.061	-116.022	7.1	17 00 00.1
7	Bourbon	37.100	-116.004	5.6	17 40 04.4
8	Bronze	37.098	-116.033	5.3	17 00 00.0
9	Buff	37.073	-116.029	5.0	19 15 00.0
10	Charcoal	37.078	-116.017	4.5	17 12 00.0
11	Chinchilla	37.049	-116.029	1.5	16 30 00.1
12	Dormouse	37.047	-116.039	3.6	18 00 00.1
13	Dormouse Prime	37.044	-116.024	2.6	18 00 00.1
14	Fisher	37.046	-116.028	3.6	23 04 59.6
15	Haymaker	37.042	-116.035	4.1	18 00 00.1
16	Hyrax	37.044	-116.021	2.2	17 10 00.1
17	Merrimac	37.055	-116.033	4.2	16 00 00.2
18	Mink	37.049	-116.031	1.9	18 30 00.1
19	Packrat	37.046	-116.039	2.6	17 00 00.1
20	Pampas	37.042	-116.029	3.6	19 10 00.1
21	Peba	37.055	-116.029	2.4	17 00 00.1
22	Ringtail	37.043	-116.025	3.6	16 35 00.1
23	Stoat	37.045	-116.035	3.0	16 30 00.1
24	Tan	37.068	-116.035	5.6	14 00 00.0
25	Wagtail	37.064	-116.037	7.5	19 13 00.0

(Table I continued)

Pahute Mesa Events

1	Boxcar	37.296	-116.456	13.2	15 00 00.0
2	Benham	37.231	-116.474	14.0	16 30 00.0
3	Chartreuse	37.348	-116.322	6.7	15 00 00.1
4	Duryea	37.243	-116.431	5.5	14 13 43.1
5	Halfbeak	37.316	-116.299	8.8	22 15 00.1
6	Greeley	37.302	-116.408	12.3	15 30 00.1
7	Palanquin	37.280	-116.524	0.9	22 15 00.1
8	Rex	37.272	-116.434	6.7	15 55 07.0
9	Scotch	37.275	-116.370	10.0	14 00 00.0
10	Scroll	37.338	-116.376	2.3	17 01 30.0
11	Knickerbocker	37.248	-116.480	6.3	15 00 00.0

Rainier Mesa Events

1	Chena	37.194	-116.207	2.6	18 00 00.0
2	Antler	37.188	-116.208	4.0	17 00 00.1
3	Feather	37.195	-116.208	2.5	16 30 00.1
4	Des Moines	37.222	-116.162	2.0	21 00 00.1
5	Madison	37.169	-116.206	4.0	17 25 00.1
6	Yuba	37.197	-116.209	2.4	17 00 00.1
7	Clearwater	37.198	-116.229	5.5	17 00 00.1
8	Red-Hot	37.174	-116.208	4.3	18 15 00.1

Frenchman Flat Events

1	Diluted Waters	36.818	-115.956	2.0	16 30 00.2
2	Pinstripe	36.888	-115.941	3.0	18 38 00.1
3	Wishbone	36.818	-115.949	1.8	16 18 47.2

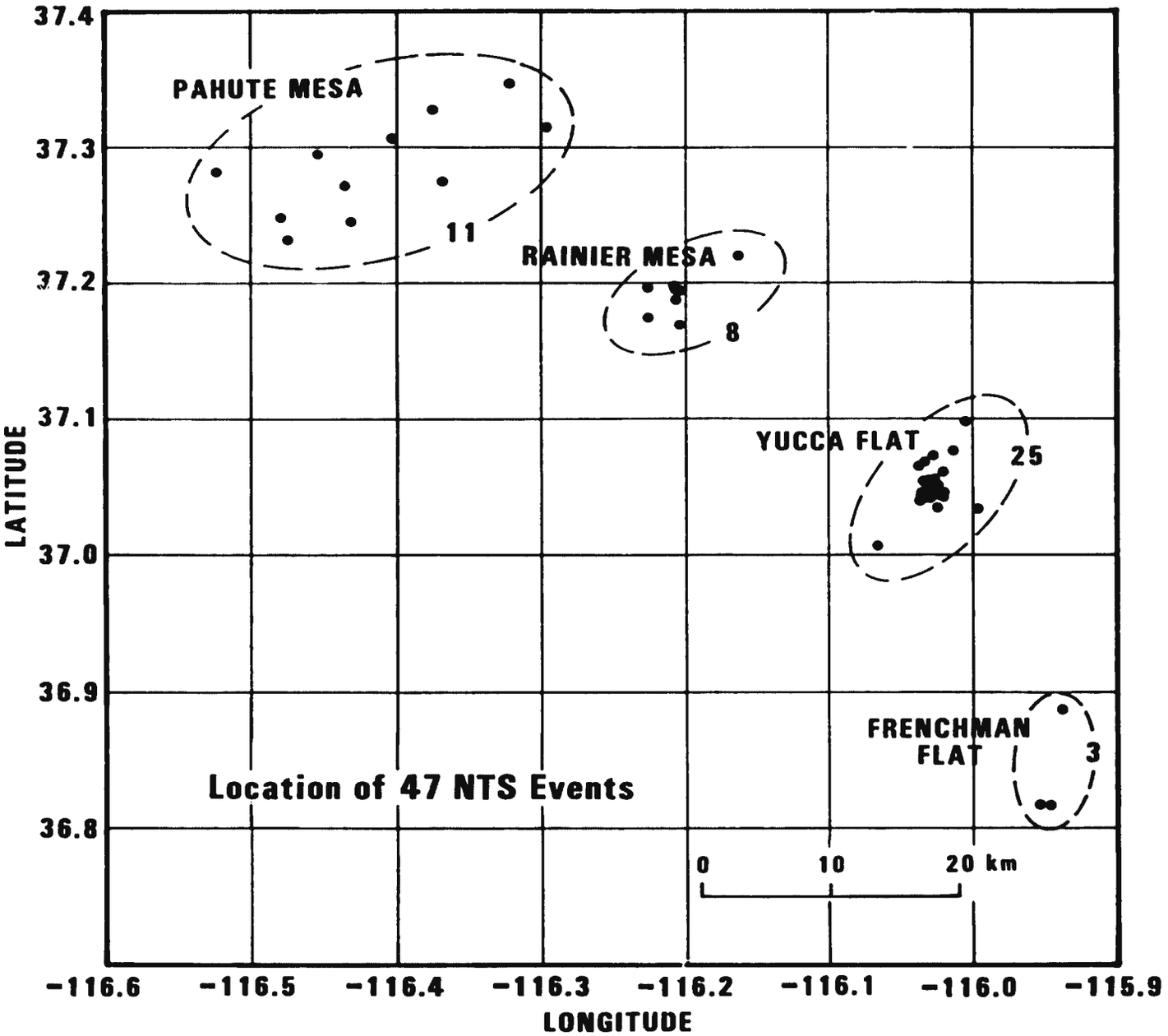

Figure 2 Location of 47 NTS explosions in four regions

2.2. Computation Method

We assume that the correlation coefficients for the arrival time residuals of Pg and Pn are a function of distance between two stations in the forms of

$$\rho_{P_n} = A_{P_n} \exp\left[\frac{-r_{ij}^2}{\Delta_{P_n}^2}\right] \tag{4}$$

and

$$\rho_{P_g} = A_{P_g} \exp\left[\frac{-r_{ij}^2}{\Delta_{P_g}^2}\right] \tag{5}$$

where A_{P_n} and A_{P_g} are correlation coefficients at the same station (i.e., distance = 0°), r_{ij} is the distance between stations i and j, and Δ_{P_n} and Δ_{P_g} are the distance where the value of ρ becomes 1/e. The adequacy of this Gaussian distance-dependent formula has not been rigorously tested. Our objective is to determine values of A and Δ for Pn and Pg. In addition, we must determine standard errors for these phases. We will also test the adequacy of the above formula.

Shumway (1980) developed a maximum likelihood estimator of distance dependent covariance functions. This method was used by Davison (1983) to estimate correlation functions for teleseismic P. Results of this investigation using travel time residuals obtained from fifteen (15) nuclear explosions show a great scatter in values : $0.1 < A_P < 0.8$, and $1° < \Delta_P < 20°$. The average value of all 15 events are $A_P = 0.47 \pm 0.24$, and $\Delta_P = 8.73° \pm 4.49$.

Instead of Shumway's maximum likelihood estimator method, we chose to use a direct measurement of correlation coefficients for several reasons. The coefficients are computed with a product moment formula,

$$\rho_{ij} = \frac{p}{\sigma_i \sigma_j} \tag{6}$$

where

$$p = \frac{\sum(\tau_i\tau_j)}{N} - \left[\frac{\sum(\tau_i)}{N}\right]\left[\frac{\sum(\tau_j)}{N}\right] \tag{7}$$

$$\sigma_i = \left[\frac{\sum(\tau_i^2)}{N} - \left[\frac{\sum\tau_i}{N}\right]^2\right]^{1/2} \tag{8}$$

$$\sigma_j = \left[\frac{\sum(\tau_j^2)}{N} - \left[\frac{\sum\tau_j}{N}\right]^2\right]^{1/2} \tag{9}$$

where τ_i and τ_j are travel time residuals at stations i and j.

The computation starts with computing the distance between all pairs of stations i and j, and pooling the residuals in groups of distance ranges 0.1° - 1.0°, 1.1° - 2.0°, 2.1° - 3.0°, ..., 19.1° - 20.0°. For the special case where residuals are recorded at the same station but from different events, values are pooled in the area where distance = 0°. The pooled ρ_{ij} are then plotted against the bins of distance in degrees, and relations of the forms (4) and (5) are fit to them (Figures 3 and 4).

There are several advantages to this computation. First, we can check the adequacy of the distance dependent formula and make corrections if necessary. Second, this routine can be modified to compute the single-station correlation coefficient of Pn and Pg. The modified program will check if the same station had reported both Pn and Pg arrivals, and if so, pool Pn residuals in τ_i and Pg residuals in τ_j. Thirdly, the computation of $\rho_{P_nP_g}$ yields σ_{P_n} and σ_{P_g} as a by-product.

2.3. Computation Results

During the computation of ρ_{ij} we discovered that many true residuals were obviously wrong, sometimes exceeding 15 seconds. This was rather unexpected because NTS shots were recorded with advance notices, and even after the recording the analyst picked signals with

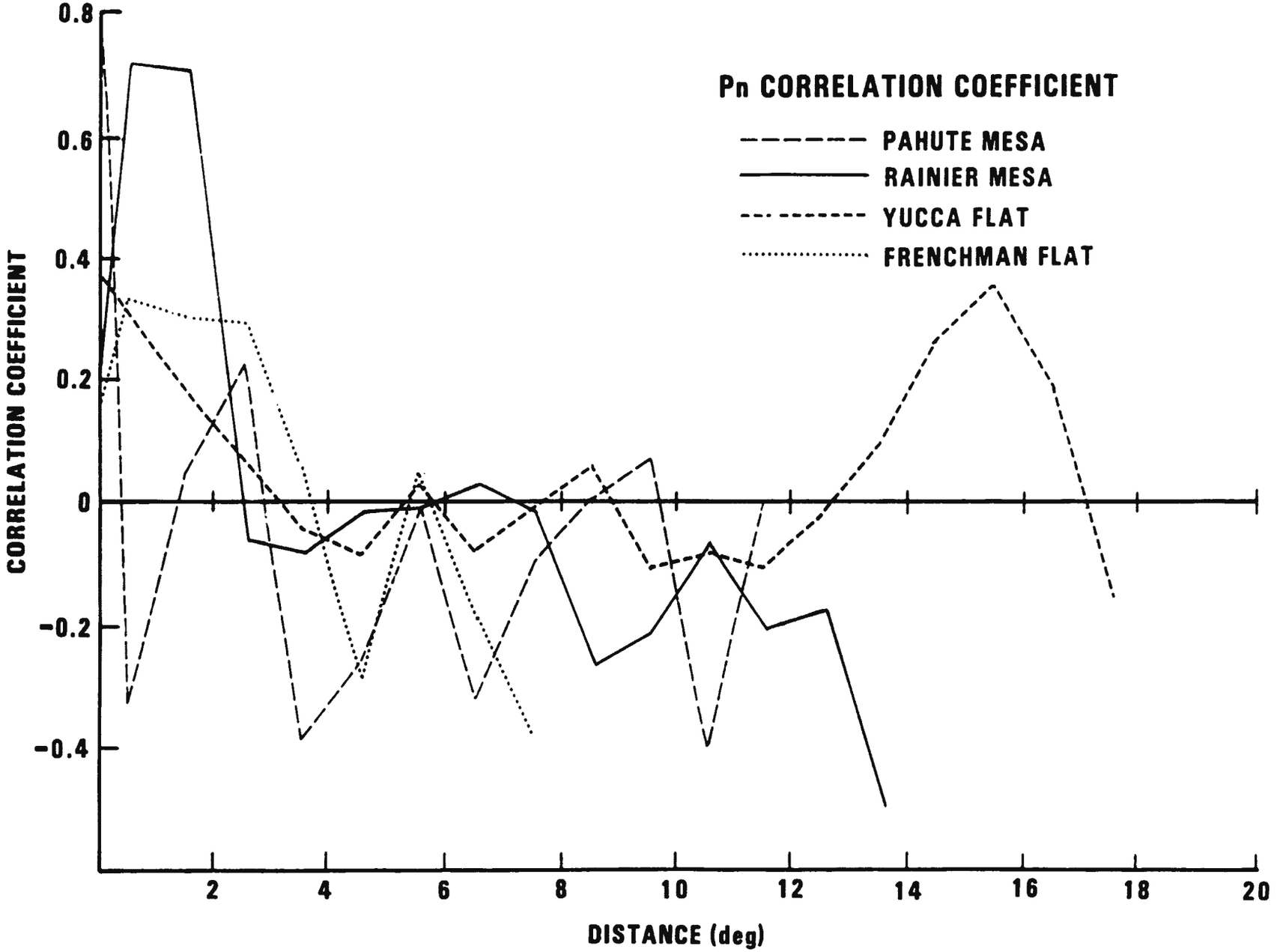

Figure 3 Correlation coefficients of Pn in four NTS regions

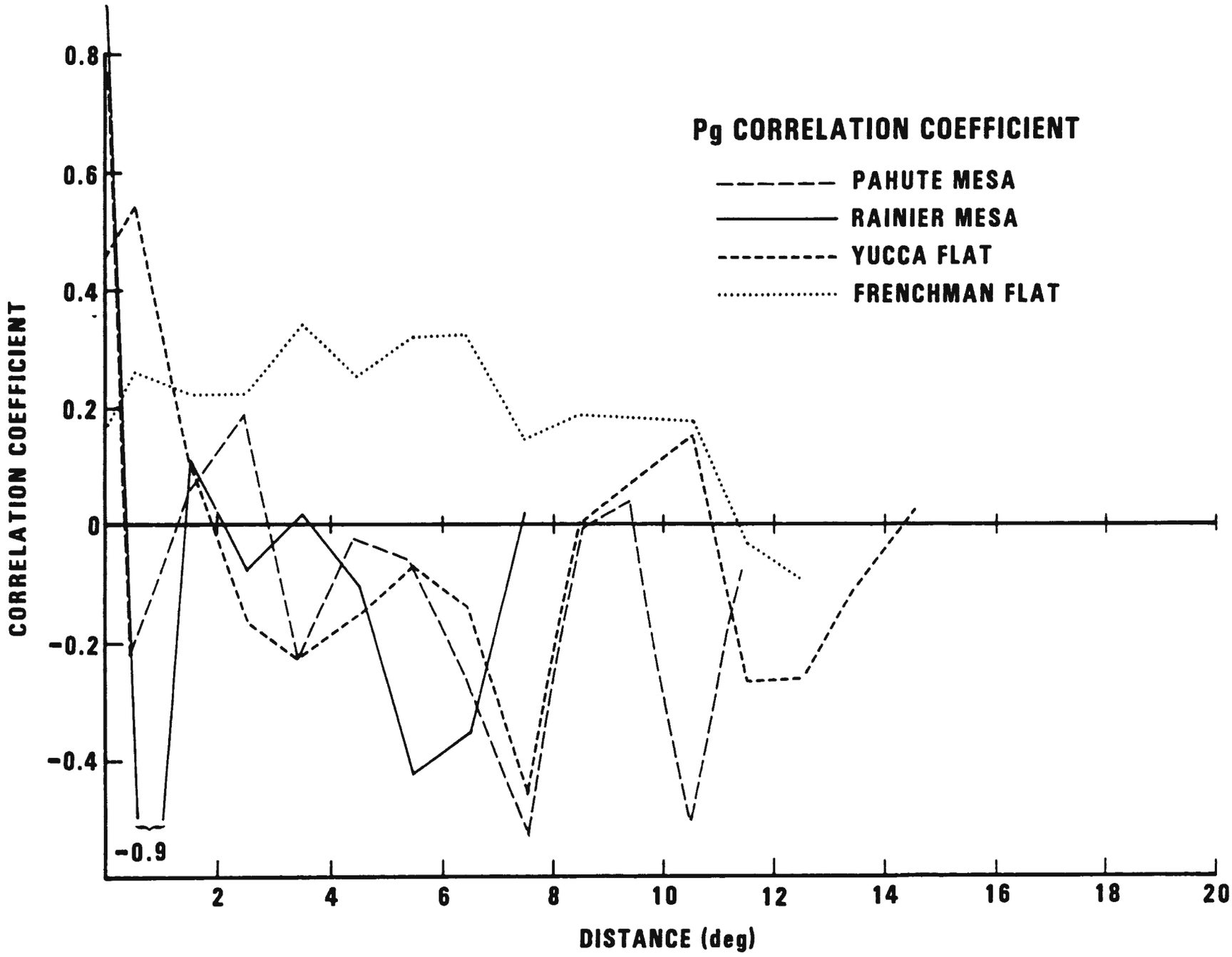

Figure 4 Correlation coefficients of Pg in four NTS regions

known distance and origin time. At any rate, since these exceptionally high residuals were clearly wrong and misleading, a time limit was set to exclude these bad residuals from computations. The computation was repeated by setting the limit to 10 seconds, 8 seconds and 5 seconds. Results are shown here for computations with the limit set to 5 seconds. By setting the limit lower, the number of samples become smaller, but the alternative is adding unreliable samples to the computation.

Correlation coefficients for Yucca Flat, Frenchman Flat, Rainier Mesa and Pahute Mesa events are presented in Figures 3 and 4. Some results are rather unexpected. In the ρ_{P_n} computations (Figure 3), the only smooth curve observed was for the Yucca Flats events, perhaps because this group has the greatest number of events. There are only 3 events in the Frenchman Flat group, so the result may not be reliable. But in the Pahute Mesa group, the correlation coefficient was 0.8 at 0°, -0.33 at 1°, and then positive again for distances greater than 1° . On the other hand, Rainier Mesa events had correlation coefficients of 0.22 at 0° and then above 0.7 in the 1° and 2° range. The poor correlations for the Pahute and Rainer Mesa events are most likely due to the complex geology under these areas.

Similarly, the Pg correlation coefficients (Figure 4) for both Pahute and Rainier Mesa events showed a strong correlation at 0° and immediately become strongly negative at the 1° range. It is clear that both Pn and Pg signals are poorly correlated because of the complex geological structures under the source region, and that the effect is more significant in Pg than in Pn, because the complexity is mostly within the crust.

The curves tend to become smoother when there are more samples. In Figure 5, correlation coefficients computed with combined groups are plotted and compared with the theoretical curves from equations (4) and (5) obtained by varying the parameters A_P and Δ_P to represent the data best. The combined groups are: (a) Pahute and Rainier Mesa events, (b) Yucca and

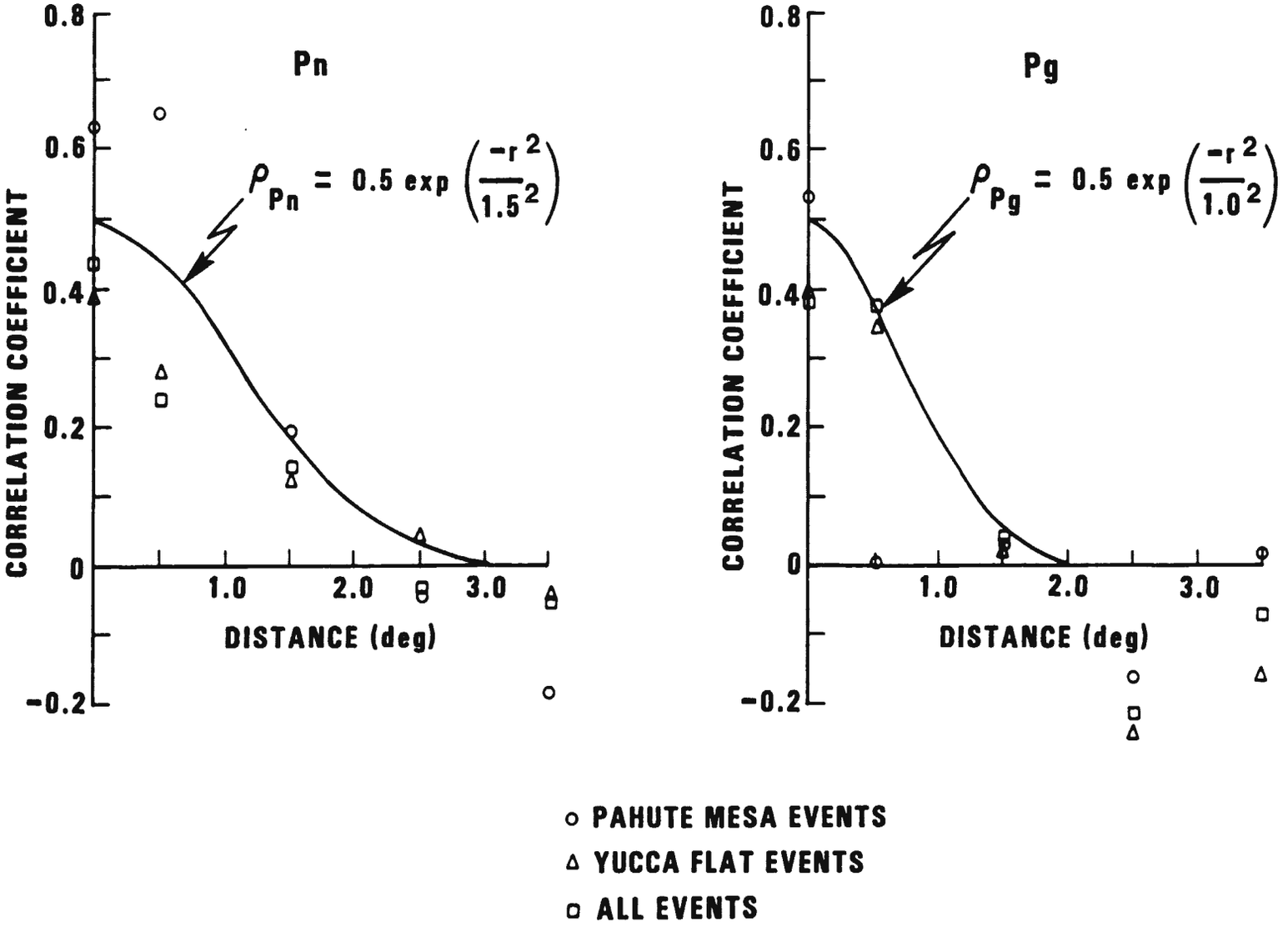

Figure 5 Computed ρ_{P_n} and ρ_{P_g} for combined regions with comparison to theoretical distance dependent curves

Frenchman Flat events and (c) all events. Horizontal scales are expanded to examine the curve more closely. Figure 5 shows that equations (4) and (5) adequately express the distance dependence of the correlation coefficients. The result shows that A_{P_n} and A_{P_g} are both about 0.5 at 0°, but the decay is faster for Pg, which goes to zero at 2°. The correlation coefficient for Pn goes to zero at 3°.

2.4. Correlations Between Pn and Pg, and Standard Errors

There are only a small number of stations that reported both Pn and Pg arrivals. However, these two phases are the most likely phases reported at the same station. Computations are made with three groups: (a) Pahute and Rainier Mesa events, (b) Yucca and Frenchman Flat events, and (c) all events. Results of this computation are shown in Table II.

TABLE II
Correlation Coefficients and Standard Errors of Pn and Pg

Regions	No. Stations	$\rho_{P_nP_g}$	σ_{P_n}	σ_{P_g}
(No Restriction)				
Pahute & Rainier	43	0.309	1.281	4.978
Yucca & Frenchman	81	0.095	2.323	3.860
All Events	124	0.145	2.024	4.306
(10 second limit)				
Pahute & Rainier	34	0.150	1.082	2.612
Yucca & Frenchman	68	0.334	1.876	3.171
All Events	102	0.297	1.656	3.002
(5 second limit)				
Pahute & Rainier	21	0.333	0.892	1.126
Yucca & Frenchman	33	-0.053	0.593	1.777
All Events	54	0.061	0.771	1.559

The standard errors showed large differences by setting no residual limit, 10 second and 5 second residual limits. On the other hand, cross correlations are less than 0.333 in all cases.

This result is somewhat unexpected because it means that Pn and Pg are not correlated at both the same station and event. From the fact that σ_{P_g} is about twice as large as σ_{P_n}, one can infer that that the crust is more heterogeneous than the upper mantle, and that the heterogeneities of crust and upper mantle are rather independent of each other.

We found that there has not been an investigation of standard errors of Pn and Pg residuals in the past. The only reference we found is the work of McCowan and Needham (1978), who "assigned" errors of observations to 11 seismic phases while relocating three explosions. Their assigned values are $\sigma_{P_n} = 1.0$, and $\sigma_{P_g} = 3.0$. Although their values are very close to our results, those values were simply estimates, and there has been no follow-up study of the matter.

3. RELOCATION EXPERIMENTS

3.1. Eliminating Bad Arrivals

As we pointed out earlier, some arrivals were apparently in error, because travel time residuals were greater than 10 seconds. A simple method to eliminate bad arrivals would be to set a rigid limit, say 10 second, in the program. But a better way is to set a "probable error" limit with 2σ, so each seismic phase will be checked against different limit settings. Assuming that signal arrivals are normally distributed, rejecting bad arrivals with residuals greater than 2σ will pass 90% of the signals as being legitimate. It is also important to point out that we do not want to purge the "bad" arrivals permanently, because the location determination is an iterative process. Our modification was to check and eliminate bad arrivals in each iteration, but those "excluded" arrivals will be re-checked in the next iteration.

During the relocation experiments, we have relocated and compared all 47 events using all three values of $\rho_{P_nP_g}$, σ_n, and σ_g shown in Table II. The first set of values, $\sigma_{P_n} = 2.0$ and $\sigma_{P_g} = 4.3$, were too lenient in setting limits, so that too many bad arrivals were still included. However, by setting $\sigma_{P_n} = 0.771$ and $\sigma_{P_g} = 1.559$ we found that too many arrivals were eliminated during computations, resulting in no solutions. By setting $\sigma_{P_n} = 1.7$ sec and $\sigma_{P_g} = 3.0$ sec, we obtained the best results.

3.2. Full and Partial Inversions

The standard technique for locating seismic events, at both regional and teleseismic distances, involves assuming a trial value of the hypocenter and origin time, calculating predicted arrival times at a set of stations for signals originating at the trial hypocenter, expanding the travel time residual at the i^{th} station, $\delta t_i = t_{i,obs} - t_{i,calc}$, in the first-order Taylor series,

$$\delta t_i = (\frac{\partial t}{\partial T})_i dT + (\frac{\partial t}{\partial x})_i dx + (\frac{\partial t}{\partial y})_i dy + (\frac{\partial t}{\partial h})_i dh, \tag{10}$$

forming a system of such equations for all residuals δt_i, solving for the location corrections dT, dx, dy, and dh by means of matrix inversion and then adding these corrections to the assumed values of the event's origin time, east, north, and depth coordinates. In order to evaluate the derivatives in this equation, one may set

$$\frac{\partial t}{\partial T} = 1 \tag{11}$$

$$\frac{\partial t}{\partial x} = \frac{\partial t}{\partial \Delta} \cdot \frac{\partial \Delta}{\partial x} = - \sin \zeta_0 \cdot \frac{\partial t}{\partial \Delta} \tag{12}$$

$$\frac{\partial t}{\partial y} = \frac{\partial t}{\partial \Delta} \cdot \frac{\partial \Delta}{\partial y} = - \cos \zeta_0 \cdot \frac{\partial t}{\partial \Delta} \tag{13}$$

where ζ_0 is the azimuth from the epicenter to the station. If the travel time relations are accurately known, then the derivatives $\frac{\partial t}{\partial \Delta}$ and $\frac{\partial t}{\partial h}$ may be calculated at the distance Δ_i and the matrix inversion thereby made tractable. Since travel times of Pn and Pg are linear, we can define them as

$$t_{P_n} = T + a_{P_n}(h) + b_{P_n} \cdot \Delta \tag{14}$$

$$t_{P_g} = T + a_{P_g}(h) + b_{P_g} \cdot \Delta \tag{15}$$

In these expressions we have made it explicit that the coefficients a_{P_n} and a_{P_g} are depth dependent, since they represent the delay between the event origin time and the first motion at the surface. The travel time residuals at regional distances may be expressed as

$$(\delta t_{P_n})_i = \left[\frac{\partial t_{P_n}}{\partial T}\right]_i dT + \left[\frac{\partial t_{P_n}}{\partial x}\right]_i dx + \left[\frac{\partial t_{P_n}}{\partial y}\right]_i dy + \left[\frac{\partial t_{P_n}}{\partial a_{P_n}}\right]_i da_{P_n} + \left[\frac{\partial t_{P_n}}{\partial b_{P_n}}\right]_i db_{P_n} \tag{16}$$

$$(\delta t_{P_g})_i = \left[\frac{\partial t_{P_g}}{\partial T}\right]_i dT + \left[\frac{\partial t_{P_g}}{\partial x}\right]_i dx + \left[\frac{\partial t_{P_g}}{\partial y}\right]_i dy +$$

$$\left[\frac{\partial t_{P_g}}{\partial a_{P_g}}\right]_i da_{P_g} + \left[\frac{\partial t_{P_g}}{\partial b_{P_g}}\right]_i db_{P_g} . \qquad (17)$$

These expressions are not explicitly a function of depth, since the depth dependence is contained within the coefficients a_{P_n} and a_{P_g}. Evaluation of the derivatives in these expressions is straightforward:

$$\frac{\partial t_{P_n}}{\partial T} = \frac{\partial t_{P_g}}{\partial T} = \frac{\partial t_{P_n}}{\partial a_{P_n}} = \frac{\partial t_{P_g}}{\partial a_{P_g}} = 1 \qquad (18)$$

$$\frac{\partial t_{P_n}}{\partial x} = -\sin \zeta_0 \cdot \left[\frac{\partial t_{P_n}}{\partial \Delta}\right] = -\sin \zeta_0 \cdot b_{P_n} \qquad (19)$$

$$\frac{\partial t_{P_g}}{\partial x} = -\sin \zeta_0 \cdot b_{P_g} \qquad (20)$$

$$\frac{\partial t_{P_n}}{\partial y} = -\cos \zeta_0 \cdot \left[\frac{\partial t_{P_n}}{\partial \Delta}\right] = -\cos \zeta_0 \cdot b_{P_n} \qquad (21)$$

$$\frac{\partial t_{P_g}}{\partial y} = -\cos \zeta_0 + b_{P_g} \qquad (22)$$

$$\left[\frac{\partial t_{P_n}}{\partial b_{P_n}}\right]_i = \Delta_i \qquad (23)$$

$$\left[\frac{\partial t_{P_g}}{\partial b_{P_g}}\right]_i = \Delta_i . \qquad (24)$$

The addition of the travel time residuals δt_{P_n}, δt_{P_g}, and δt_{L_g} to the conventionally calculated residuals δt_P enables the event location to be expressed in terms of an expanded set of coordinates (x, y, h, T, a_{P_n}, b_{P_n}, a_{P_g}, b_{P_g}, a_{L_g}, b_{L_g}). For an over-determined system of more than ten observations, a solution (in the least-squares sense) may be found for the newly defined ten-dimensional hypocenter in the same manner as a solution would normally be found for the four-dimensional hypocenter, as is outlined by Julian (1973).

If there are no observations of teleseismic P, then the system of equations does not involve h explicitly and so the depth cannot be determined. Similarly, the absence of Pn, Pg or Lg arrival time data means that the matrix manipulation must be carried out in a six (or eight) dimensional subspace by restraining the unmeasured coefficients.

In addition to this automatic restraining of the unmeasured phase, the program is provided with an option to restrict any parameter, a_{P_n}, b_{P_n}, a_{P_g}, b_{P_g}, a_{L_g} and b_{L_g}. This allowed us to experiment with yet another option, namely to restrain a_{P_n} and a_{P_g} in the inversion process. This was prompted by the result of relocating events with the Simultaneous Inversion Method (SIMUL), that both a_{P_n} and a_{P_g} were oftentimes erroneous. Because these parameters are functions of depth, the resulting depth estimates for the event location were wrong. Note that in the inversion process, a_{P_n} and a_{P_g} may not turn out the same depth. This will cause the least-squares process to turn out erroneous results because the travel times of Pn and Pg are now computed with two different depths. By restraining a_{P_n} and a_{P_g} to time delays computed on the basis of an *a priori* estimate of the depth, we obtain Pn and Pg velocities which are then used to calculate travel times using equations (14) and (15). However, this restriction does not prevent us from subsequently determining the event depth h *a posteriori* in the least-squares solution. We call this option Partial Simultaneous Inversion (PSIMUL), while the conventional option is called Full Simultaneous Inversion (FSIMUL). The PSIMUL option is very much like the Successive Determinations Method (SUCCESS) described in Section 1.2.3, where Pn and Pg velocities are updated through successive iterations. The traditional location method with using one Earth model is called NSIMUL for no simultaneous inversions.

The Covariance Matrix Method (COVMTX) can be used together with the above three options. This leads to a total of six different options to be tested : (1) FSIMUL and COVMTX, (2) FSIMUL and no COVMTX, (3) PSIMUL and COVMTX, (4) PSIMUL and no

COVMTX, (5) NSIMUL and COVMTX, and (6) NSIMUL and no COVMTX. Option (6) is the traditional method.

3.3. Relocation Results

All 47 events were relocated with the six options stated above. The results of absolute location errors are shown in Table III for comparison. Simplified option codes are: FS+CO, FS+NC, PS+CO, PS+NC, NS+CO, NS+NC for the six options explained in the previous section. As was explained in section 2.4 and 3.1, results shown in Table III are computed with $\sigma_{P_n} = 1.7$ sec and $\sigma_{P_g} = 3.0$ sec.

TABLE III
Comparison of Absolute Location Errors Using Six Options

Yucca Flat Events

Name	FS+CO	FS+NC	PS+CO	PS+NC	NS+CO	NS+NC
Aardvark	# 37.330	24.706	5.495	5.409	7.772	7.727
Acushi *	3.757	3.987	4.871	5.032	6.782	+ 7.275
Agouti *	1.084	0.988	3.092	3.045	3.936	3.769
Armadilo	321.494	327.935	# 19.831	# 19.617	17.699	13.767
Auk	12.910	12.588	5.585	5.290	6.949	6.806
Bilby	# 31.072	# 32.397	4.450	5.067	4.003	4.430
Bourbon	54.467	54.454	12.893	12.921	12.941	12.928
Bronze	12.320	18.742	5.217	+ 5.735	5.227	6.696
Buff	# 50.790	# 52.988	14.520	11.564	4.595	3.015
Charcoal	8.992	12.963	2.132	4.634	5.564	4.110
Chinchilla *	1.054	0.815	1.246	1.114	2.066	2.047
Dormouse *	4.790	4.732	4.220	4.010	6.065	4.569
Dormouse Prime *	1.850	1.865	2.273	2.237	3.702	1.822
Fisher *	0.663	1.074	0.804	2.453	2.131	2.021
Haymaker	22.600	24.245	1.095	2.917	1.156	1.515
Hyrax *	4.692	4.684	5.436	5.457	6.817	6.809
Merrimac	23.928	24.882	1.894	11.012	6.260	6.297
Mink *	2.332	2.349	4.337	4.328	8.934	8.924
Packrat *	4.704	4.701	4.516	5.350	5.700	5.715
Pampas *	2.334	2.386	2.348	2.726	3.121	3.260
Peba	38.965	38.954	3.989	10.793	10.887	10.860
Ringtail *	6.853	7.271	4.061	5.745	5.620	5.707
Stoat *	1.492	1.952	0.899	1.487	1.485	1.635
Tan	28.437	28.443	5.119	4.056	4.436	5.127
Wagtail	21.468	22.638	6.776	5.109	7.920	6.997

Notes:
* Depth Restricted Events
# True location lies outside 3-D ellipsoid, but inside 2-D ellipse
+ True location lies inside 3-D ellipsoid, but outside 2-D ellipse
! True location lies outside of both 3-D ellipsoid and 2-D ellipse
& True location lies outside of the 2-D ellipse in a depth restricted run

Table III Continued

Pahute Mesa events

Name	FS+CO	FS+NC	PS+CO	PS+NC	NS+CO	NS+NC
Boxcar	# 40.438	# 40.235	2.083	2.149	2.790	2.412
Benham	20.068	29.075	11.626	11.608	5.587	5.587
Chartreuse	# 45.125	# 43.765	8.343	9.438	5.959	6.800
Duryea	# 42.114	# 42.581	9.499	8.918	10.625	10.534
Greeley	30.034	29.782	14.463	14.377	7.256	8.654
Halfbeak	29.939	37.516	13.023	14.340	9.993	10.953
Palanquin	# 53.209	# 53.013	+ 18.067	+ 16.566	3.915	3.226
Rex	# 54.505	# 53.383	11.560	11.039	9.158	9.659
Scotch	37.430	37.447	15.601	15.485	2.249	2.425
Scroll	2.264	2.313	2.719	2.657	4.468	4.286
Knickerbocker	101.813	101.902	14.537	14.523	10.503	10.420

Rainier Mesa Events

Name	FS+CO	FS+NC	PS+CO	PS+NC	NS+CO	NS+NC
Antler *	2.114	2.088	2.342	2.348	1.515	1.526
Chena *	5.858	5.819	3.472	3.442	3.883	3.885
Feather *	3.291	3.735	6.655	7.424	18.557	18.458
Madison *	4.133	4.101	2.975	3.008	0.854	1.023
Yuba *	3.936	3.755	3.629	3.447	0.738	0.737
Clearwater *	6.037	6.953	6.211	7.096	& 10.694	& 13.561
Red Hot *	3.259	3.158	2.734	2.639	4.784	4.525
Des Moines *	1.184	1.732	0.460	0.491	0.605	0.655

Frenchman Flat Events

Name	FS+CO	FS+NC	PS+CO	PS+NC	NS+CO	NS+NC
Wishbone	17.670	18.813	10.439	! 9.248	20.685	21.474
Diluted Waters	5.118	# 73.401	+ 3.046	2.971	2.998	4.028
Pinstripe	49.220	49.904	9.652	9.670	14.894	15.059

TABLE IV
Average Location Errors In NTS Regions

Name	FS+CO	FS+NC	PS+CO	PS+NC	NS+CO	NS+NC
Yucca Flat	28.016	28.508	5.106	5.888	6.071	5.752
Pahute Mesa	41.308	42.817	11.047	11.009	6.608	6.814
Rainier Mesa	3.805	3.918	3.560	3.737	5.204	5.546
Frenchman Flat	23.993	47.373	7.712	7.296	12.859	113.520
All Events	26.801	28.876	6.399	6.810	6.482	6.462

Location errors averaged over each region and over all events are shown in Table IV. In this table we generally find that the COVMTX method gives a small improvement over the runs without the COVMTX method. In overall performance we find that PS+CO gives the best result.

The FSIMUL option performed poorly, because the inversions for a_{P_n} and a_{P_g} lead to erroneous depth estimates. With the exception of the Pahute Mesa region, PSIMUL gave better location estimates than the traditional location method (NS option).

In the FSIMUL option we found that some location errors were over 100 kilometers. They were all depth errors, sometimes too deep and sometimes above the ground. These depth errors were caused by errors in a_{P_n} and a_{P_g}. It clearly shows that the inversion for depth is not accurate. Comparing the results for the PSIMUL option where the a-coefficients were not inverted, we see that the results improved when the a values were restrained, resulting in the option with the smallest errors.

The COVMTX method was tested with three other options, FSIMUL, PSIMUL and NSIMUL. Results showed that on the average the use of the Covariance Matrix Method did not show significant improvements in location estimates. Because both Pn and Pg are poorly correlated, there is no location bias due to station clustering. It is important to point out that if clustered events or stations are poorly correlated, as turns out to be the case for this data set,

then the Joint Event Determination Method (JED) designed by Douglas (1967) will perform poorly.

3.4. Confidence Ellipses

Since the COVMTX method will remove biases due to station clusters, confidence ellipses will have smaller aspect ratios. Figures 6 to 14 show a comparison of confidence ellipses with and without using the COVMTX method. In these figures we present confidence ellipses for 3 Frenchman Flat events processed with the six options. Comparisons are made to examine whether the COVMTX method made any difference in the aspect ratio. Results show although differences are small, ellipses using the COVMTX method have aspect ratios closer to 1.

Examination of Table III also shows whether the true locations lie outside of the 3-D error ellipsoid or the 2-D error ellipse. We note that locations using the FSIMUL option resulted in 9 cases for which the true location was found outside the 3-D ellipsoid but inside the 2-D ellipse. This was due to erroneous depths resulting from the simultaneous inversion for a_{P_n} and a_{P_g}. In these cases the use of the COVMTX method did not put the true location back into the ellipsoid. In fact, throughout all the events we found only four cases where the use of the COVMTX method put the true locations inside the ellipsoid while results without the COVMTX method put them outside. This result may not be conclusive, but since Herrin 68 travel times are quite adequate to locate events in Western United States, we think this result indicates that the PC+CO solutions provide the best results for any generalized conditions of locating seismic events. It is also important to point out that there were several cases where the true locations were outside the error ellipses when located without COVMTX, but they were found inside the error ellipses with COVMTX.

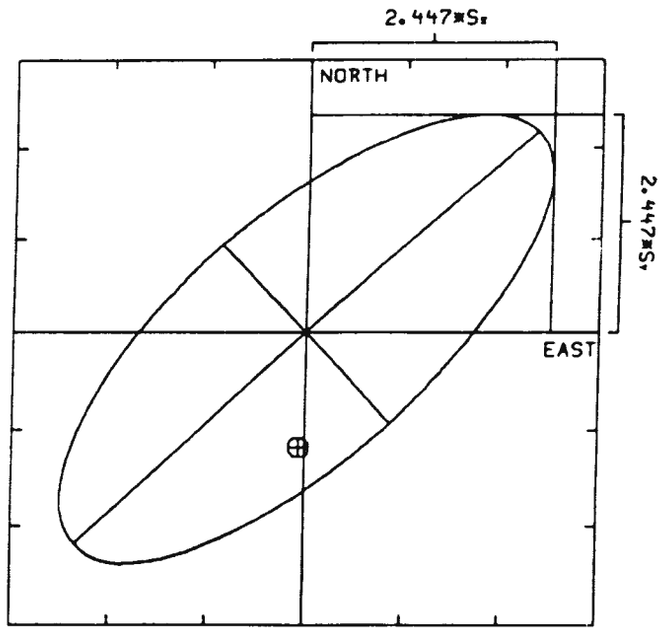

Sx: STANDARD ERROR (EAST) ⊕ TRUE EPICENTER
Sy: STANDARD ERROR (NORTH) ⊢——⊣ 9.226 KM

ELLIPSE IS FOR CHI-SQUARED STATISTIC

ERROR ELLIPSES FOR WISBON, FSIM, YCOV

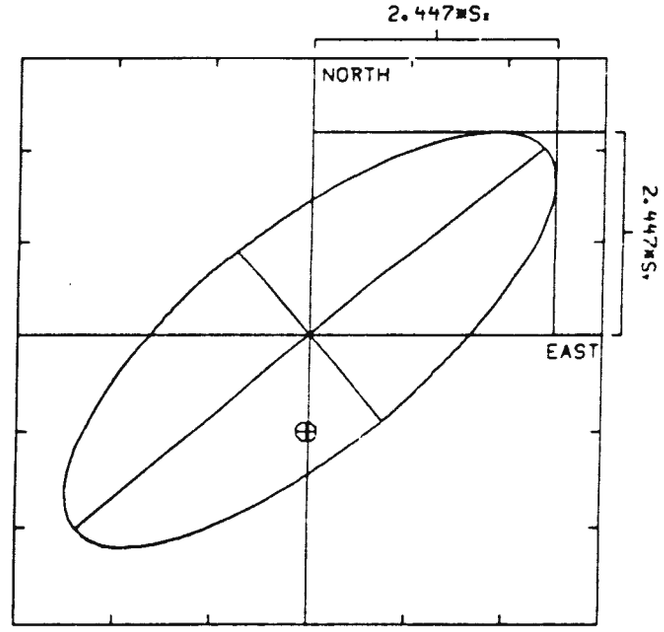

Sx: STANDARD ERROR (EAST) ⊕ TRUE EPICENTER
Sy: STANDARD ERROR (NORTH) ⊢——⊣ 9.158 KM

ELLIPSE IS FOR CHI-SQUARED STATISTIC

ERROR ELLIPSES FOR WISBON, FSIM, NCOV

Figure 6 Comparison of error ellipses before and after applying COVMTX method to event Wishbone, using FSIMUL

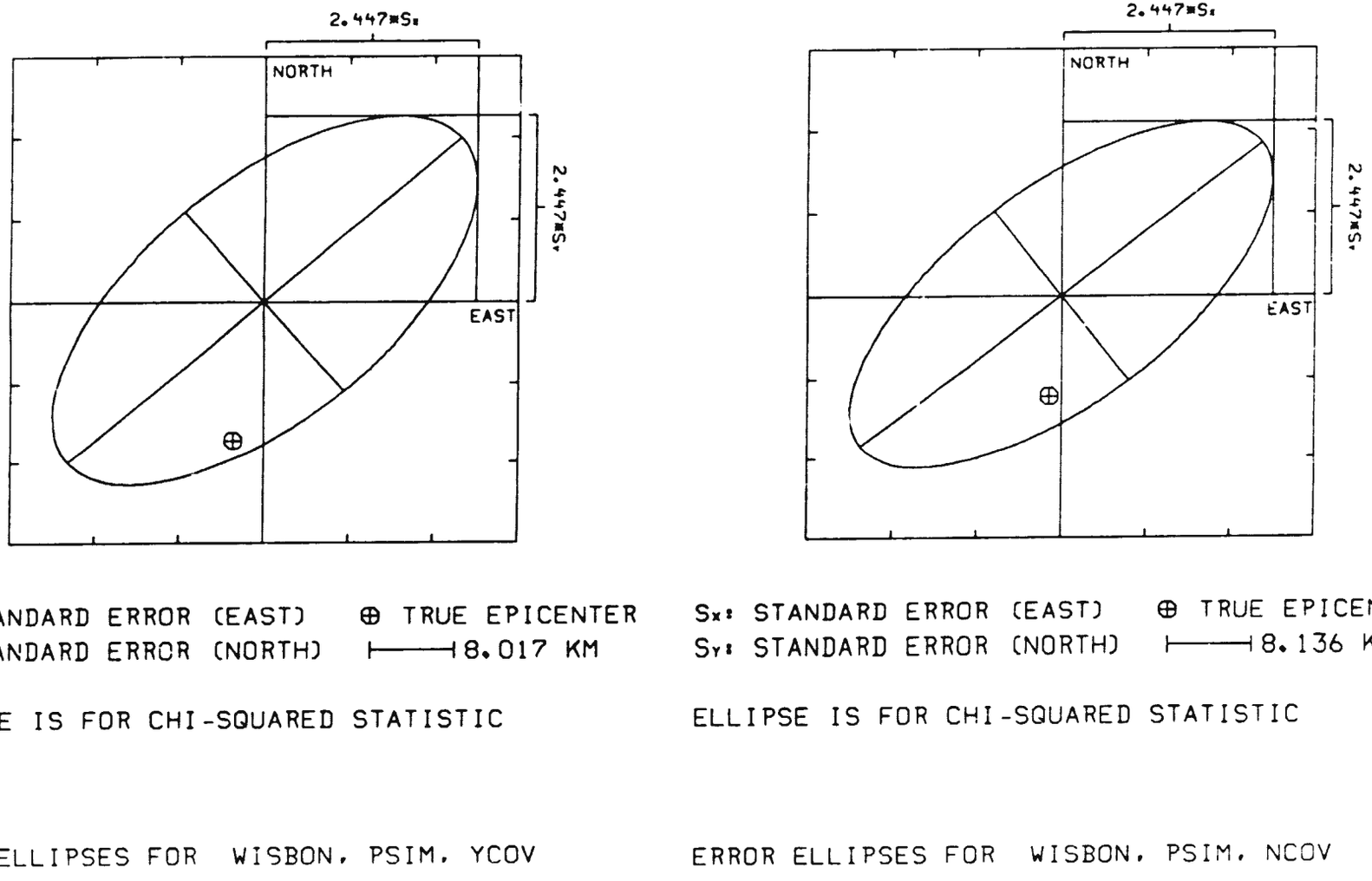

Figure 7 Comparison of error ellipses before and after applying COVMTX method to event Wishbone, using PSIMUL

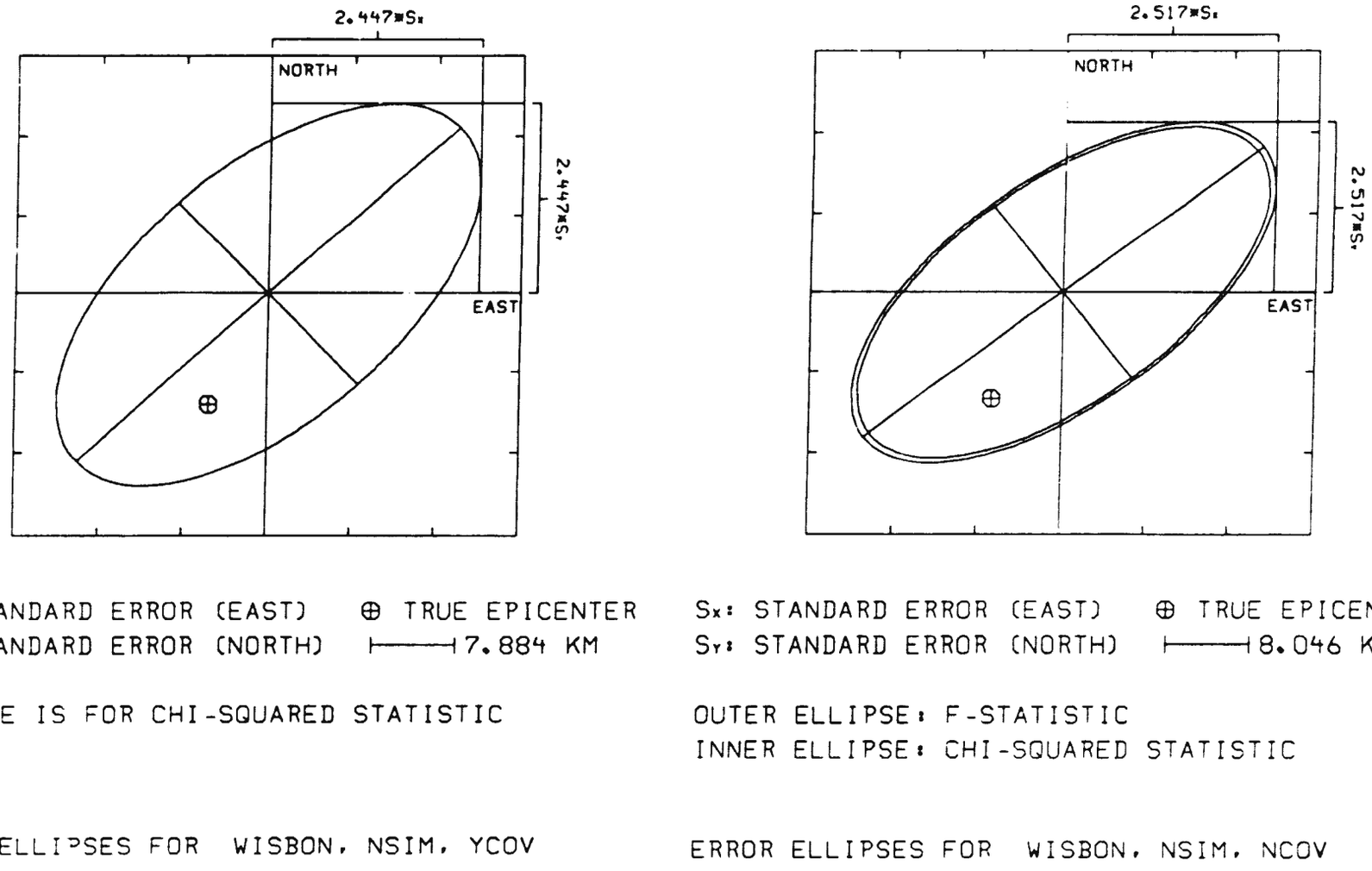

Figure 8 Comparison of error ellipses before and after applying COVMTX method to event Wishbone, using conventional method (NSIMUL)

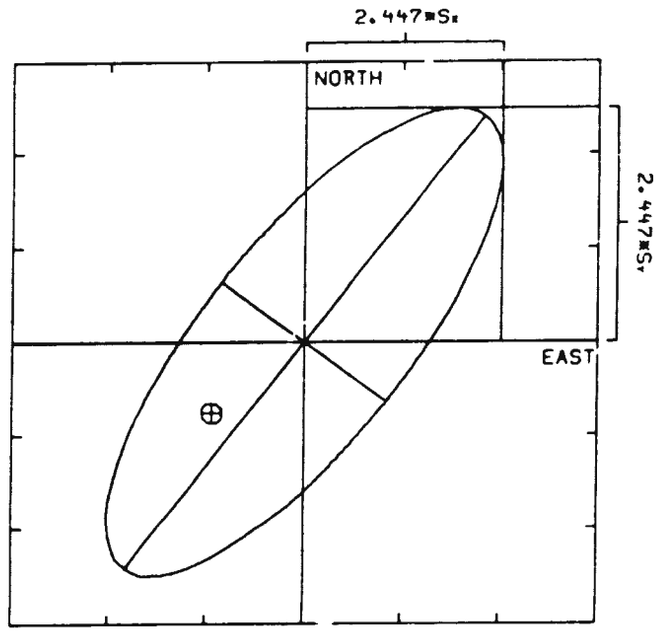

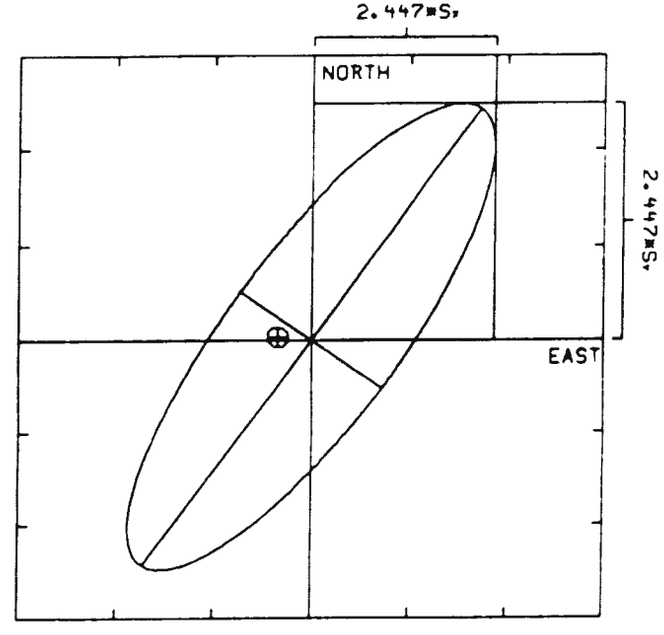

Figure 9 Comparison of error ellipses before and after applying COVMTX method to event Pinstripe, using FSIMUL

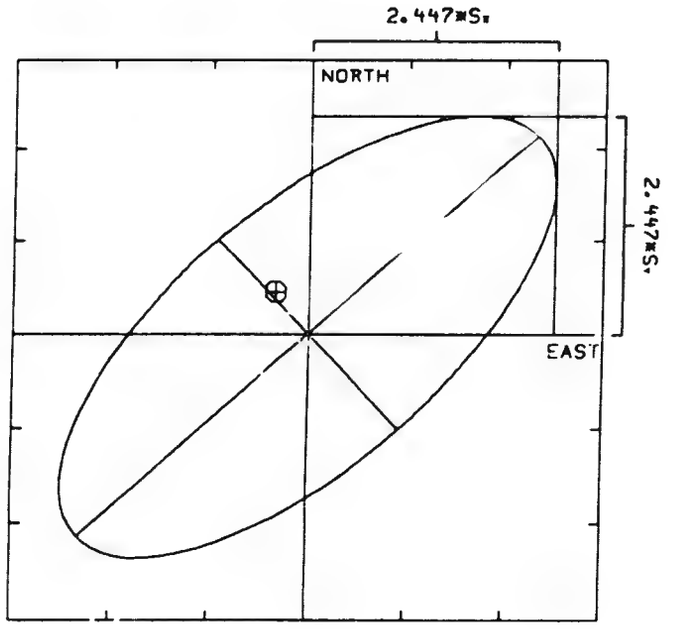

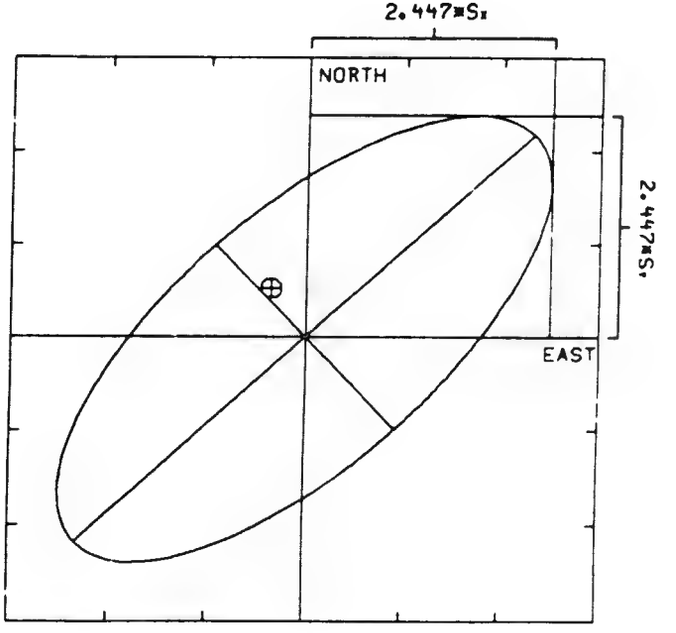

Sx: STANDARD ERROR (EAST) ⊕ TRUE EPICENTER
Sy: STANDARD ERROR (NORTH) ⊢——⊣ 6.973 KM

ELLIPSE IS FOR CHI-SQUARED STATISTIC

ERROR ELLIPSES FOR PINSTR, PSIM, YCOV

Sx: STANDARD ERROR (EAST) ⊕ TRUE EPICENTER
Sy: STANDARD ERROR (NORTH) ⊢——⊣ 6.818 KM

ELLIPSE IS FOR CHI-SQUARED STATISTIC

ERROR ELLIPSES FOR PINSTR, PSIM, NCOV

Figure 10 Comparison of error ellipses before and after applying COVMTX method to event Pinstripe, using PSIMUL

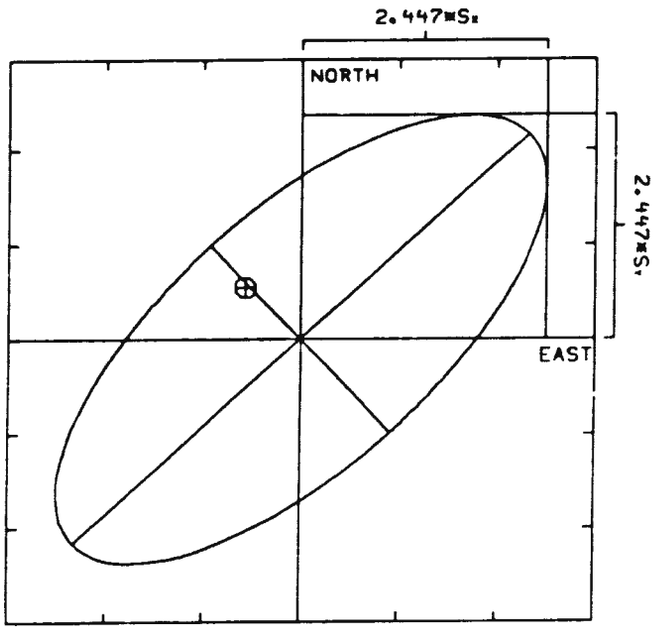

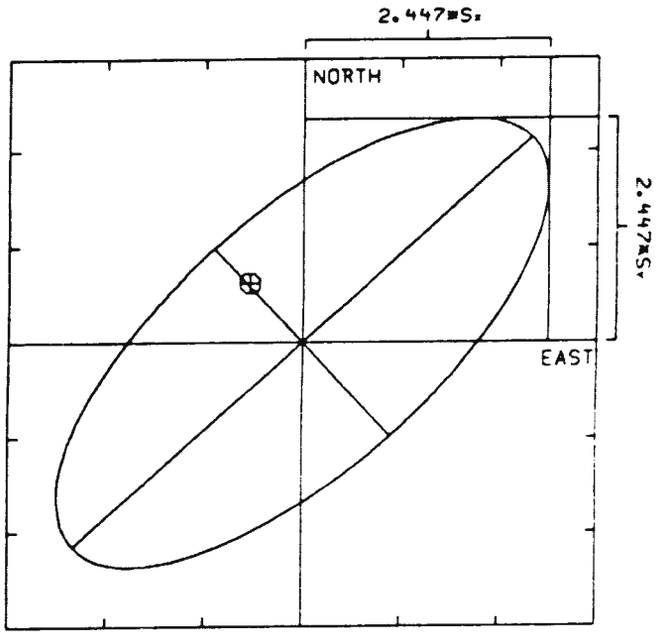

Sx: STANDARD ERROR (EAST) ⊕ TRUE EPICENTER
Sy: STANDARD ERROR (NORTH) ⊢——⊣ 6.861 KM

ELLIPSE IS FOR CHI-SQUARED STATISTIC

ERROR ELLIPSES FOR PINSTR, NSIM, YCOV

Sx: STANDARD ERROR (EAST) ⊕ TRUE EPICENTER
Sy: STANDARD ERROR (NORTH) ⊢——⊣ 6.864 KM

ELLIPSE IS FOR CHI-SQUARED STATISTIC

ERROR ELLIPSES FOR PINSTR, NSIM, NCOV

Figure 11 Comparison of error ellipses before and after applying COVMTX method to event Pinstripe, using conventional method (NSIMUL)

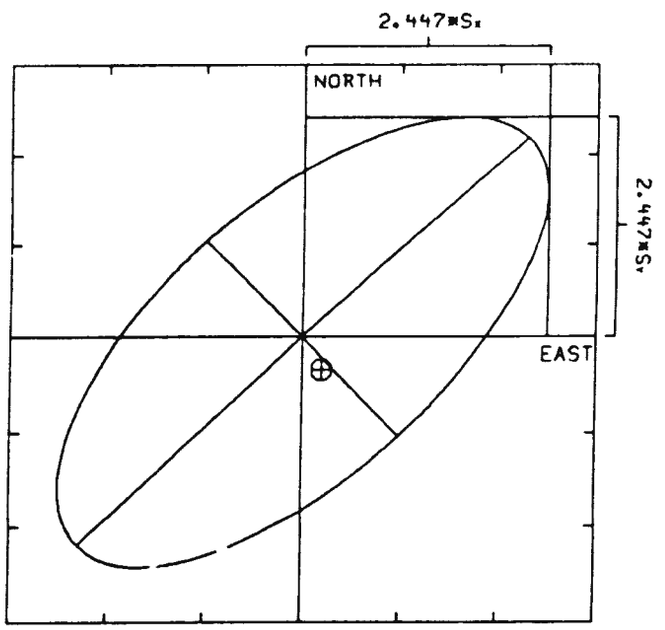

Sx: STANDARD ERROR (EAST) ⊕ TRUE EPICENTER
Sy: STANDARD ERROR (NORTH) ⊢——⊣ 8.767 KM

ELLIPSE IS FOR CHI-SQUARED STATISTIC

ERROR ELLIPSES FOR DILWAT, FSIM, YCOV

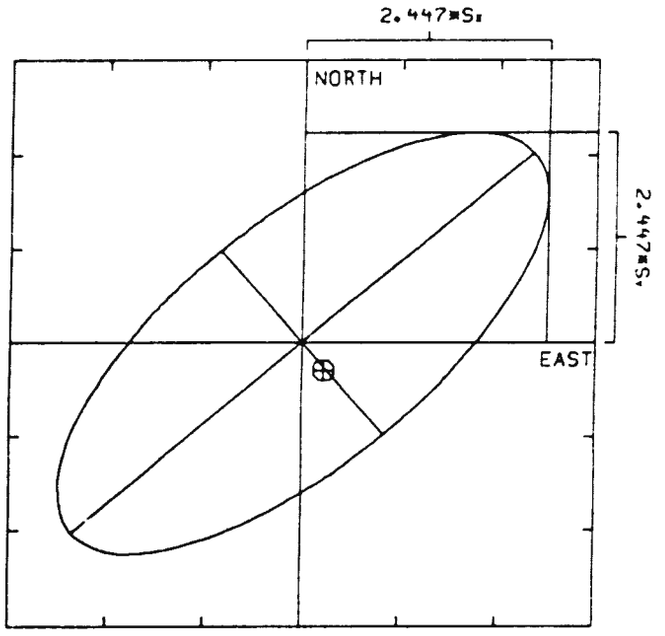

Sx: STANDARD ERROR (EAST) ⊕ TRUE EPICENTER
Sy: STANDARD ERROR (NORTH) ⊢——⊣ 8.698 KM

ELLIPSE IS FOR CHI-SQUARED STATISTIC

ERROR ELLIPSES FOR DILWAT, FSIM, NCOV

Figure 12 Comparison of error ellipses before and after applying COVMTX method to event Diluted Waters, using FSIMUL

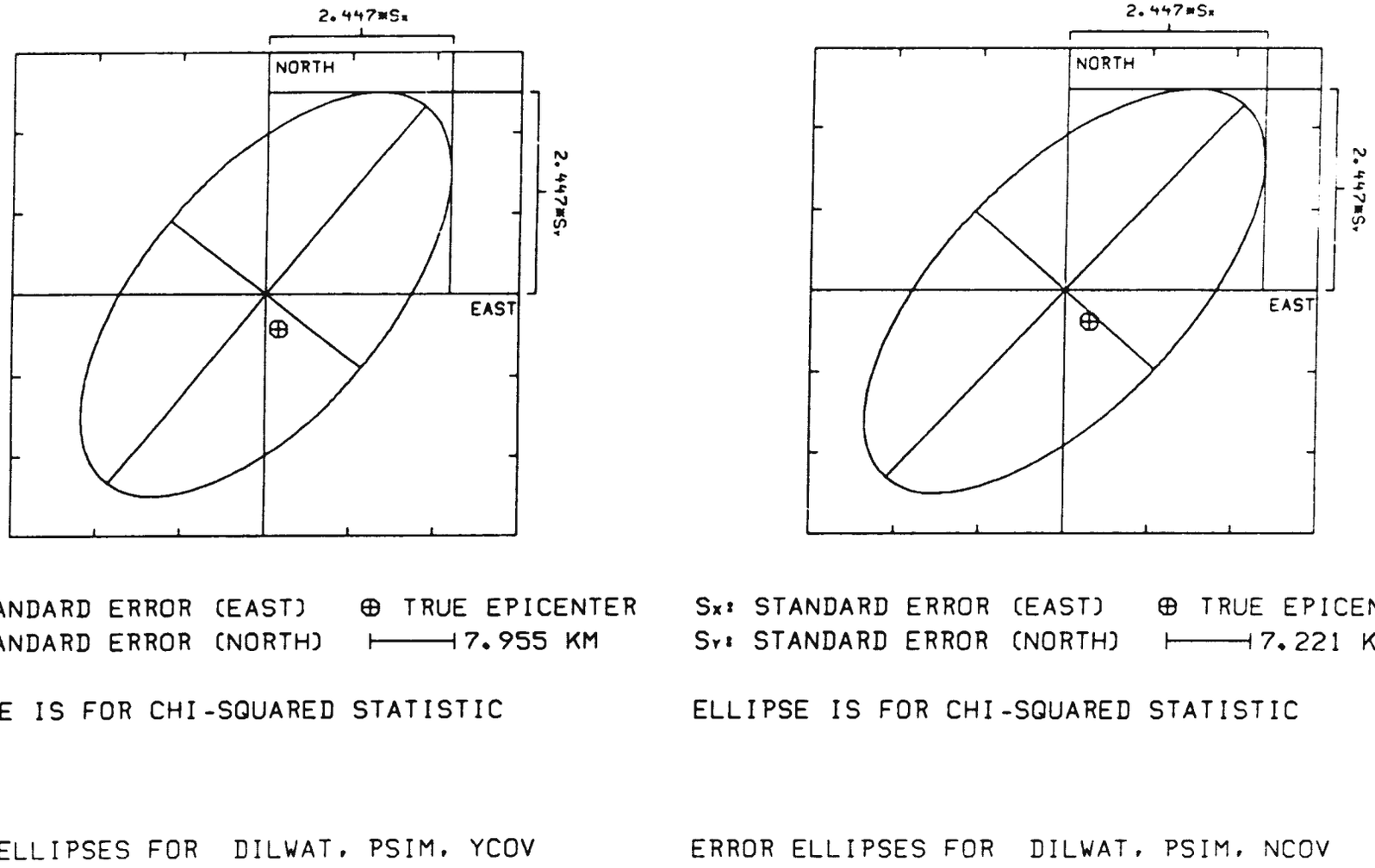

Figure 13 Comparison of error ellipses before and after applying COVMTX method to event Diluted Waters, using PSIMUL

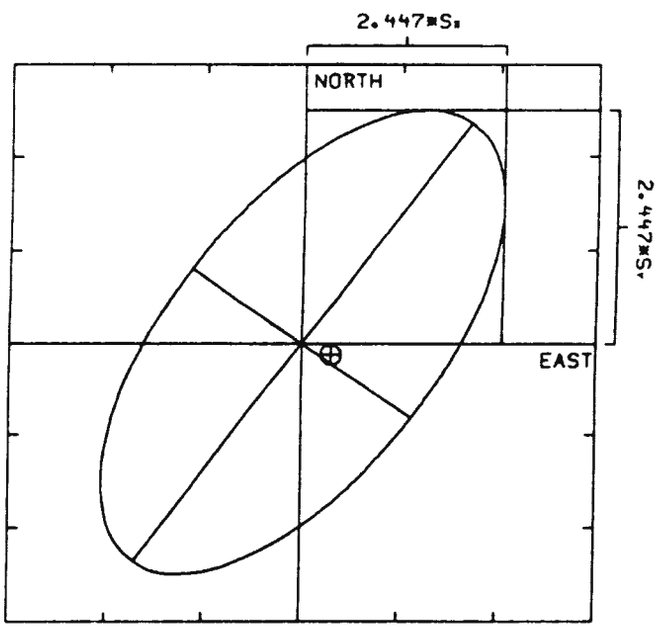

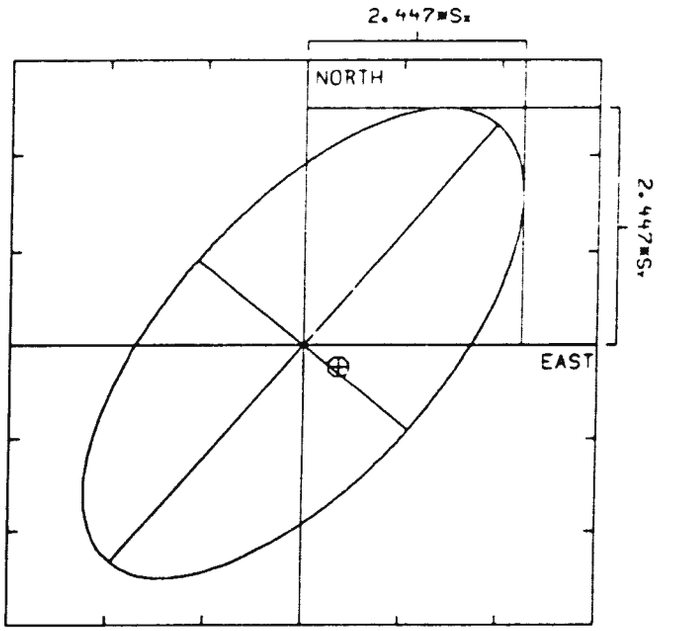

Figure 14 Comparison of error ellipses before and after applying COVMTX method to event Diluted Waters, using conventional method (NSIMUL)

4. SUMMARY AND CONCLUSIONS

This investigation was conducted using 47 NTS explosions to determine Pn and Pg correlation coefficients ρ_{P_n}, ρ_{P_g}, $\rho_{P_nP_g}$, and standard deviations, σ_{P_n} and σ_{P_g}. All events were relocated using six options and three different settings of σ_{P_n} and σ_{P_g}. We shall now summarize the principal findings.

* Correlation coefficients of Pn and Pg residuals follow the formula

$$\rho_{P_n} = 0.5 \exp\left[-\left[\frac{r_{ij}}{1.5}\right]^2\right] \tag{25}$$

and

$$\rho_{P_g} = 0.5 \exp\left[-\left[\frac{r_{ij}}{1.0}\right]^2\right] \tag{26}$$

for $i \neq j$, and $\rho_{P_n} = \rho_{P_g} = 1.0$ for $i = j$. Here the inter-station separation r_{ij} is measured in degrees.

* Pn and Pg arrival times received at the same station from same event are not correlated.

* Standard errors of Fn and Pg arrival time residuals were determined to be $\sigma_{P_n} = 1.7$ sec and $\sigma_{P_g} = 3.0$ sec respectively.

* An option to examine bad arrivals in each iteration was added to the location program by excluding those residuals exceeding 2σ of the population.

* Full simultaneous inversion gave poor depth estimates and thus resulted in greater location errors. Partial simultaneous inversion gave the best results.

* Although the PSIMUL + COVMTX method did not improve location estimates significantly over the conventional method, the method is expected to give consistent results for any area, whereas the conventional method may not work as well in other areas because it can not update Pn and Pg velocities.

Finally, we note that there may be some future for the use of later phases such as Lg, S, PP, PPP, PcP etc., with the Successive Determinations Method approach. The reasons why these phases were not used in the past lies in the fact that there are no reliable travel time tables and that local variations of travel times for these phases are significantly larger than are those for P, Pn or Pg. Application of the Successive Determinations Method to develop travel times of these phases, and properly weighting each phase by using the COVMTX method, may provide new possibilities for using those later phases.

5. ACKNOWLEDGEMENT

The author benefited in this work from several discussions with W. Rivers and R. Shumway. T. McElfresh assisted in the installation of the old confidence ellipse routine.

6. REFERENCES

Chang, A. C. and D. P. J Racine (1979). Evaluation of location accuracy using Pn and Pg arrivals, SDAC-TR-79-4, Teledyne Geotech, Alexandria, Virginia.

Chang, A. C., D. W. Rivers and J. A. Burnetti (1981). Improved location with regional events. VSC-TR-81-10, Teledyne Geotech, Alexandria, Virginia.

Chang, A. C., R. H. Shumway, R. R. Blandford and B. W. Barker (1983). Two methods to improve location estimates - Preliminary results. Bull. Seism. Soc. Am., 73, 281-295.

Davison, G. E. (1983). Correlation of residual time data in earthquake epicenter location methods. Old Dominion University, Norfolk, Virginia.

Douglas, A (1973). Joint epicenter determination, Nature, 215, 47.

Flinn, E. A., E. R. Engdahl and A. R. Hill (1974). Seismic and Geographical Regionalization. Bull. Seism. Soc. Am., 64, Number 3 Part II.

Julian, R. R. (1973). Extension of standard event location procedures, Seismic Discrimination SATS, Lincoln Laboratory, M.I.T., 30 June 1973.

McCowan, D. W. and R. E. Needham (1978). The use of crustal phases in locating explosion epicenters. Seismic Discrimination SATS, Lincoln Laboratory, M.I.T., 9 June 1978.

Shumway, R. H. (1980). Estimation of parameters in distance dependent models for the covariance matrix of location residuals. Internal Memorandum, Teledyne Geotech, Alexandria, Virginia.

(THIS PAGE INTENTIONALLY LEFT BLANK)

DISTRIBUTION LIST
DARPA-FUNDED PROJECTS
(UNCLASSIFIED REPORTS)
(Last Revised: 3 Sep 85)

RECIPIENT	COPIES
DEPT. OF DEFENSE	
DARPA/GSD 1400 Wilson Boulevard Arlington, VA 22209	2
DARPA/PM 1400 Wilson Boulevard Arlington, VA 22209	1
Defense Intelligence Agency Directorate for Scientific and Technical Intelligence Washington, D.C. 20301	1
Defense Nuclear Agency Shock Physics Directorate/SS Washington, D.C. 20305	1
Defense Technical Information Center Cameron Station Alexandria, VA 22314	12
DEPT. OF AIR FORCE	
AFGL/LW ATTN: Dr. J. Cipar Terrestrial Sciences Division Hanscom AFB, MA 01730	1
AFOSR/NPG ATTN: Director Bldg 410, Room C222 Bolling AFB, Washington D.C. 20332	1
AFTAC/CA (STINFO) Patrick AFB, FL 32925-6001	1
AFTAC/TG Patrick AFB, FL 32925-6001	4
AFWL/NTESC Kirtland AFB, NM 87171	1

DEPT. OF THE NAVY

NORDA
ATTN: Dr. J. A. Ballard
Code 543
NSTL Station, MS 39529 — 1

DEPT. OF ENERGY

Department of Energy
ATTN: Dr. R. Ewing (DP-52)
International Security Affairs
1000 Independence Avenue
Washington, D.C. 20545 — 1

Lawrence Livermore National Laboratory
ATTN: Dr. J. Hannon and Dr. M. Nordyke
University of California
P.O. Box 808
Livermore, CA 94550 — 2

Los Alamos Scientific Laboratory
ATTN: Dr. K. Olsen
P.O. Box 1663
Los Alamos, NM 87544 — 1

Sandia Laboratories
ATTN: Mr. P. Stokes
Geosciences Department 1255
Albuquerque, NM 87115 — 1

OTHER GOVERNMENT AGENCIES

Central Intelligence Agency
ATTN: Dr. L. Turnbull
OSI/NED, Room 5G48
Washington, D.C. 20505 — 1

U.S. Arms Control and Disarmament Agency
ATTN: Dr. M. Eimer
Verification and Intelligence Bureau, Rm 4953
Washington, D.C. 20451 — 1

U.S. Arms Control and Disarmament Agency
ATTN: Mrs. M. Hoinkes
Multilateral Affairs Bureau, Rm 5499
Washington, D.C. 20451 — 1

U.S. Geological Survey
ATTN: Dr. T. Hanks
National Earthquake Research Center
345 Middlefield Road
Menlo Park, CA 94025 — 1

U.S. Geological Survey
ATTN: Dr. R. Masse
Global Seismology Branch
Box 25046, Stop 967
Denver Federal Center
Denver, CO 80225 — 1

UNIVERSITIES

University of California, Berkeley
ATTN: Dr. T. McEvilly
Department of Geology and Geophysics
Berkeley, CA 94720 — 1

California Institute of Technology
ATTN: Dr. D. Harkrider
Seismological Laboratory
Pasadena, CA 91125 — 1

University of California, San Diego
ATTN: Dr. J. Orcutt
Scripps Institute of Oceanography
La Jolla, CA 92093 — 1

Columbia University
ATTN: Dr. L. Sykes
Lamont-Doherty Geological Observatory
Palisades, NY 10964 — 1

Massachusetts Institute of Technology
ATTN: Dr. S. Soloman, Dr. N. Toksoz, Dr. T. Jordan
Department of Earth and Planetary Sciences
Cambridge, MA 02139 — 3

The Pennsylvania State University
ATTN: Dr. S. Alexander
Department of Mineral Sciences
University Park, PA 16802 — 1

Southern Methodist University
ATTN: Dr. E. Herrin
Geophysical Laboratory
Dallas, TX 75275 — 1

CIRES
ATTN: Dr. C. Archambeau
University of Colorado
Boulder, CO 80309 — 1

St. Louis University
ATTN: Dr. O. Nuttli
Department of Earth and Atmospheric Sciences
3507 Laclede
St. Louis, MO 63156 — 1

DEPT. OF DEFENSE CONTRACTORS

Applied Research Associates, Inc.
ATTN: Dr. N. Higgins
2101 San Pedro Boulevard North East
Suite A
Albuquerque, NM 87110 — 1

Applied Theory, Inc.
ATTN: Dr. J. Trulio
930 South La Brea Avenue
Suite 2
Los Angeles, CA 90036 — 1

Center for Seismic Studies
ATTN: Dr. C. Romney and Mr. R. Perez
1300 N. 17th Street, Suite 1450
Arlington, VA 22209 — 2

ENSCO, Inc.
ATTN: Mr. G. Young
5400 Port Royal Road
Springfield, VA 22151 — 1

ENSCO, Inc.
ATTN: Dr. R. Kemerait
1930 Highway A1A
Indian Harbour Beach, FL 32937 — 1

Pacific Sierra Research Corp.
ATTN: Mr. F. Thomas
12340 Santa Monica Boulevard
Los Angeles, CA 90025 — 1

R&D Associates
ATTN: Dr. E. Martinelli
P.O. Box 9695
Marina del Ray, CA 90291 — 1

Rockwell International ATTN: Dr. B. Tittman 109 Camino Dos Rios Thousand Oaks, CA 91360	1
Gould Inc. ATTN: Mr. R. J. Woodard Chesapeake Instrument Division 6711 Baymeado Drive Glen Burnie, MD 21061	1
Rondout Associates, Inc. ATTN: Dr. P. Pomeroy P.O. Box 224 Stone Ridge, NY 12484	1
Science Applications, Inc. ATTN: Dr. T. Bache P.O. Box 2351 La Jolla, CA 92038	1
Science Horizons ATTN: Dr. T. Cherry and Dr. J. Minster 710 Encinitas Blvd Suite 101 Encinitas, CA 92024	2
Sierra Geophysics, Inc. ATTN: Dr. R. Hart and Dr. G. Mellman 15446 Bell-Red Road Redmond, WA 98052	2
SRI International ATTN: Dr. A. Florence 333 Ravensworth Avenue Menlo Park, CA 94025	1
S-Cubed, A Division of Maxwell Laboratories Inc. ATTN: Dr. S. Day P.O. Box 1620 La Jolla, CA 92038	1
S-Cubed, A Division of Maxwell Laboratories Inc. ATTN: Mr. J. Murphy 11800 Sunrise Valley Drive Suite 1212 Reston, VA 22091	1

Teledyne Geotech 2
ATTN: Dr. Z. Der and Mr. W. Rivers
314 Montgomery Street
Alexandria, VA 22314

Woodward-Clyde Consulants 1
ATTN: Dr. L. Burdick
556 El Dorado St P.O. Box 932
Pasadena, CA 91109-3245

Weidlinger Associates 1
ATTN: Dr. J. Isenberg
620 Hansen Way #100
Palo Alto, CA 94304

NON-US RECIPIENTS

National Defense Research Institute 1
ATTN: Dr. Ola Dahlman
Stockholm 80, Sweden

Blacknest Seismological Center 1
ATTN: Mr. Peter Marshall
Atomic Weapons Research Establishment
UK Ministry of Defense
Brimpton, Reading RG7-4RS
United Kingdom

NTNF NORSAR 1
ATTN: Dr. Frode Ringdal
P.O. Box 51
N-2007 Kjeller
Norway

OTHER DISTRIBUTION

To be determined by the project office 9